250
2-6-78

DR 1819

ERDA/JPL/954144-77/3

SILICON RIBBON GROWTH BY A CAPILLARY ACTION SHAPING TECHNIQUE

Annual Report

Quarterly Technical Progress Report Number 9

By
G. H. Schwuttke
T. F. Ciszek
A. Kran

October 1, 1977

MASTER

Work Performed Under Contract No. NAS-7-100-954144

International Business Machines Corporation
East Fishkill Laboratories
Hopewell Junction, New York

U.S. Department of Energy

Solar Energy

DISTRIBUTION OF THIS DOCUMENT IS UNLIMITED

DISCLAIMER

This report was prepared as an account of work sponsored by an agency of the United States Government. Neither the United States Government nor any agency Thereof, nor any of their employees, makes any warranty, express or implied, or assumes any legal liability or responsibility for the accuracy, completeness, or usefulness of any information, apparatus, product, or process disclosed, or represents that its use would not infringe privately owned rights. Reference herein to any specific commercial product, process, or service by trade name, trademark, manufacturer, or otherwise does not necessarily constitute or imply its endorsement, recommendation, or favoring by the United States Government or any agency thereof. The views and opinions of authors expressed herein do not necessarily state or reflect those of the United States Government or any agency thereof.

DISCLAIMER

Portions of this document may be illegible in electronic image products. Images are produced from the best available original document.

NOTICE

This report was prepared as an account of work sponsored by the United States Government. Neither the United States nor the United States Department of Energy, nor any of their employees, nor any of their contractors, subcontractors, or their employees, makes any warranty, express or implied, or assumes any legal liability or responsibility for the accuracy, completeness or usefulness of any information, apparatus, product or process disclosed, or represents that its use would not infringe privately owned rights.

This report has been reproduced directly from the best available copy.

Available from the National Technical Information Service, U. S. Department of Commerce, Springfield, Virginia 22161.

Price: Paper Copy $6.00
Microfiche $3.00

ERDA/JPL/954144-77/3
Distribution Category UC-63

SILICON RIBBON GROWTH BY A CAPILLARY ACTION SHAPING TECHNIQUE

G. H. Schwuttke, Principal Investigator, 914 - 897 - 3140
International Business Machines Corporation
East Fishkill Laboratories
Hopewell Junction, New York 12533

NOTICE
This report was prepared as an account of work sponsored by the United States Government. Neither the United States nor the United States Department of Energy, nor any of their employees, nor any of their contractors, subcontractors, or their employees, makes any warranty, express or implied, or assumes any legal liability or responsibility for the accuracy, completeness or usefulness of any information, apparatus, product or process disclosed, or represents that its use would not infringe privately owned rights.

Annual Report
(Quarterly Technical Progress Report Number 9)
October 1, 1977

prepared by:
G. H. Schwuttke, T. F. Ciszek, and A. Kran

Under JPL Contract Number: 954144
(Subcontract under NASA Contract NAS7-100)
(Task Order No. RD-152)
Effective Date of Contract: 5/8/75
Contract Expiration Date: 11/8/77

This work was performed for the Jet Propulsion Laboratory, California Institute of Technology, under NASA Contract NAS7-100 for the U. S. Energy Research and Development Administration, Division of Solar Energy.

The JPL Low-Cost Silicon Array Project is funded by ERDA and forms part of the ERDA Photovoltaic Conversion Program to initiate a major effort toward the development of low-cost solar arrays.

DISTRIBUTION OF THIS DOCUMENT IS UNLIMITED

THIS PAGE

WAS INTENTIONALLY

LEFT BLANK

CONTENTS

CONTENTS (cont'd)

CONTENTS (cont'd)

TECHNICAL CONTENT STATEMENT

This report contains information prepared by the International Business Machines Corporation under JPL contract. Its contents are not necessarily endorsed by the Jet Propulsion Laboratory, California Institute of Technology, or by the National Aeronautics and Space Administration.

RESEARCH PROGRAM PLAN

OBJECTIVES

1. Technological assessment of ribbon growth of silicon by a capillary action shaping technique.

2. Economic evaluation of ribbon silicon grown by a capillary action shaping technique as low-cost silicon.

SYNOPSIS OF PROGRAM OF STUDY

1. Crystal growth of silicon ribbons.

2. Characterization of silicon ribbons.

3. Economic evaluations and computer-aided simulation of ribbon growth.

NINTH QUARTER HIGHLIGHTS

- A 100-mm-wide ribbon growth furnace has been installed and is in the process of being debugged.

- Vitreous carbon shows promise as a crucible material both for ribbon growth and for directional solidification.

- A crack-free 5 cm diameter silicon ingot with a grain size of several mm was directionally solidified in a vitreous carbon crucible.

- The display of defects under MOS capacitors on silicon ribbon by scanning electron microscope in electron beam induced current (EBIC) mode is described.

- The technique provides a tool for the evaluation of the electrical activity of defects according to their relative attenuating effect on the EBIC. This in turn can be used for interpretation of measured lifetime.

- If ribbon technology is to compete with Czochralski technology for $>500/kWE solar array production contracts through 1986, it must be phased into

manufacturing starting in 1978.

o The following schedule is proposed for bridging from ribbon technology development to large scale production through utilization of manufacturing science:

- Suspension of further Ribbon Technology Development:	1977/78
- Definition and Utilization of Manufacturing Science:	1978/86
- Initiate Phasing into Manufacturing:	1978
- Initial Manufacturing Technology Ready:	1980
- Pilot Production:	1980/81
- Small Scale Production (1-10 MW):	1982/84
- Large Scale Production (20-100 MW):	1985/86

o For 1986, the following sheet technology costs are projected. They are based upon the schedule (item 2), technology parameter values of Fig. 2 on page 68, and have been taken from Fig. 11 on page 81:

- $\$48/m^2$ ($320/kWE) sheet material cost appears as a good bet for 10 cm wide ribbon, $10/kg poly, 15% cell.

  Alternatives: 16.3 cm wide ribbon, $20/kg poly
  8.5 cm wide ribbon, $ 5/kg poly

- $30/m^2$ ($200/kWE) sheet material cost cannot be obtained with 10 cm wide ribbon, 15% cell, even at zero poly cost.

  Possibilities: 21.0 cm wide ribbon, $10/kg poly
  15.0 cm wide ribbon, $ 5/kg poly

- $20/m^2$ ($133/kWE) sheet material cost is unrealistic with ribbon technology defined here and considered reasonable.

  Data Point: 25.0 cm wide ribbon, $4/kg poly.

TENTH QUARTER ACTIVITY PLAN

- Complete debugging of 100 mm ribbon system and initiate growth experiments.

- Continue ribbon characterization with particular emphasis on solar cell parameters.

- Complete ribbon technology assessment: 1976-1986 (Part 2).

CRYSTAL GROWTH

by

T. F. Ciszek

1.0 INTRODUCTION

The crystal-growth method under investigation is a capillary action shaping technique. Meniscus-shaping for the desired ribbon geometry occurs at the vertex of a wettable die. As ribbon growth depletes the melt meniscus, capillary action supplies replacement material. The configuration of the technique used in our initial studies was similar to the edge-defined, film-fed growth (EFG) process described by LaBelle (1). The crystal-growth method has been applied to silicon ribbons for several years (2,3,4). As our work on silicon ribbon growth has progressed, we have found that substantial improvements in ribbon surface quality could be achieved with a higher melt meniscus than that attainable with the EFG technique. Thus, in our later work we have abandoned the EFG technique in favor of the improved capillary action shaping techique, which employs the capillary die design shown in Fig. 1.

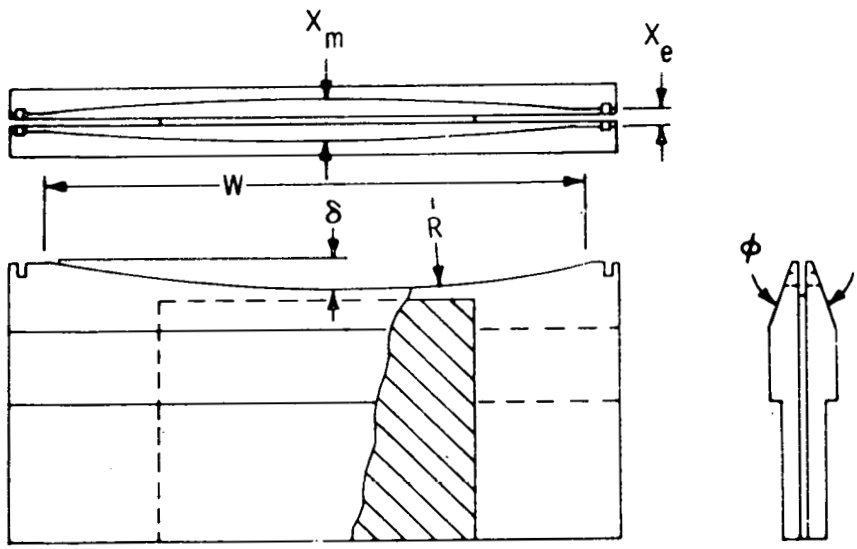

Fig. 1. Capillary Die Design

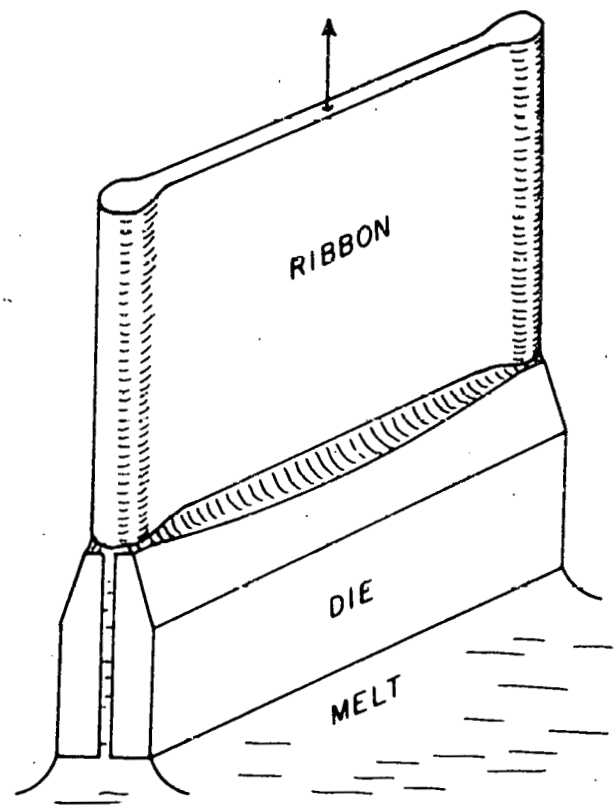

Fig. 2. CAST High Melt Meniscus Growth

It represents a departure from the die types used for edge-defined, film-fed growth, in that the bounding edges of the die top are not parallel or concentric with the growing ribbon. The new die allows a higher central melt meniscus (Fig. 2) with concomitant improvements in surface smoothness and freedom from SiC surface particles, which can degrade perfection.

Certain problems still await solution before the technique becomes viable for large-scale economical photovoltaic applications. High-density graphite fulfills the durability and wettability requirements of a die (2) and has been used, to date, for most silicon ribbon growth; it is not, however, completely non-reactive. Good crystallographic perfection has been achieved on small ribbon segments (2,3), but the structure of large ribbons is marred by planar, line, and point defects.

Our objective in this work is to attain a clear technological assessment of silicon ribbon growth by the capillary action shaping technique and to enhance the applicability of the technique to photovoltaic power device material.

In this report, our progress in scale-up of the process from

50 mm to 100 mm ribbon widths is presented, the use of vitreous carbon as a crucible material (both for ribbon growth and for directional solidification) is analyzed, and preliminary tests of CVD Si_3N_4 as a potential die material are reported.

A crack-free ingot of silicon 5 cm in diameter was directionally solidified in a vitreous carbon crucible. The resultant grain size was several millimeters.

2.0 100 mm GROWTH SYSTEM

All furnace parts have been received and assembled. Welding of watercooling channels to the furnace end pieces has been completed. A 210 mm I.D. x 210 mm high, 12 turn RF coil was fabricated and leak checked. Adaptors have been installed to accommodate the new furnace on the existing machine frame. Also, plumbing of the cooling water system, alignment of the furnace, tuning of the RF generator to the large RF coil and tuning of the temperature control system have been completed. Seeds and silicon polycrystalline charges have been sawed.

Hot zone components have been outgassed in vacuum at up to 1510°C. This required an RF generator output power of 34 KW

(9.8 KV at 3.5 amps), compared to about 9 KW for our 50 mm ribbon furnace. In attempting to melt silicon and grow ribbons in an argon atmosphere, we have so far been unsucessful because of ionization of the argon due to the high RF coil voltage. Steps are being taken to alleviate this problem. In Fig. 3, the new 100 mm furnace is shown with the old 50 mm furnace.

3.0 DIE/CRUCIBLE MATERIAL EVALUATION

3.1 Vitreous Carbon

Vitreous carbon was given a preliminary evaluation as a potential crucible material. In the same experiment, directional solidification of silicon in the crucible was achieved.

3.1.1 Experimental

a 139 gram polycrystalline charge of silicon was placed in a 50 mm diameter x 50 mm high vitreous carbon crucible along with sufficient boron to produce a 2 ohm-cm average resistivity. Graphite r-f susceptors and heat shields were arranged to establish a vertically-decreasing temperature gradient of about 35^{o}C/cm, the bottom of the crucible being

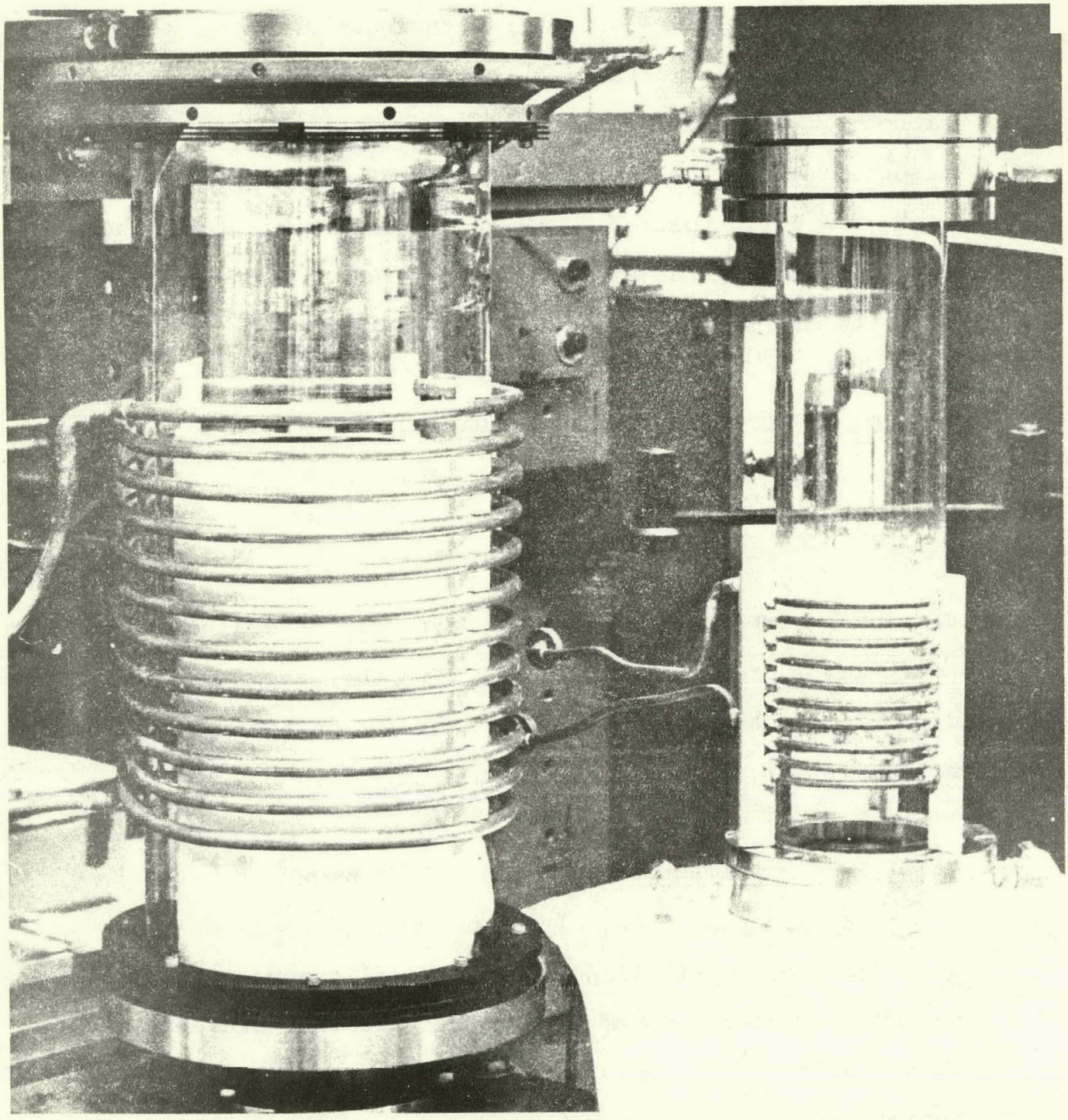

Fig. 3. 100 mm Furnace (Left) and 50 mm Furnace

the hottest region. The system first was heated to melt the silicon and then additonally heated to a temperature of 1680°C (at the top melt surface). Since the melt was about 3 cm deep, the temperature at the bottom of the crucible was approximately 1785°C. The molten silicon was held at this temperature for 15 minutes. The system temperature was then decreased at a rate of 2.5°C/min. (while maintaining the vertical gradient) until the entire charge had solidified (about 2 hours). The cooling rate was then increased to 20°C/min. until the silicon temperature was 1000°C, at which time the power was turned off. The growth system was very clear during this experiment (no silicon oxide fluff deposits as are typically present when using a quartz crucible).

3.1.2 Results

Upon removal from the furnace, the solidified silicon was found to be intact and free of cracks (Fig. 4). Several thin slices were sawed from the bottom and top of the cylindrical ingot. Small silicon carbide particles were found at the carbon/silicon interface on the crucible bottom.

At a distance of 0.7 mm from the crucible bottom, the silicon grain distribution was as shown in Fig. 5. Grain

Fig. 4. Silicon Directionally Solidified (Bottom to Top) in a Vitreous Carbon Crucible

Fig. 5. Grain Characteristics at 0.7 mm from Crucible Bottom (10X)

size ranged from 0.05 mm to 2 mm, with 0.5 mm being a typical size. The silicon here was P-type, and resistivities ranged fron 1.4-5.0 ohm-cm.

At a distance of 2.5 cm from the crucible bottom, the grains were substantially larger (Fig. 6). They ranged up to 4 mm in size, with 1 mm being a typical size. Figure 7 is a photo of the opposite side of the slice region shown in Fig. 6. The slice was 1.2 mm thick. As can be seen, there is a substantial amount of vertical boundary behaviour. Some of the grains visible from both sides of the slice are identified with corresponding numbers. The resistivity here ranged from 0.5-2.1 ohm-cm, P-type.

Since the grains are large and at least some of the boundaries are vertical, these wafers will be processed into solar cells to determine their photovoltaic suitability.

It should be noted that the grain structure of this material is very similar to that reported by Fischer and Pschunder (5) for the Wacker-Chemitronic non-single crystalline silicon upon which solar cells of up to 12.5% AMO efficiency were fabricated.

3.1.3 Discussion

Directional solidification or Bridgeman/Stockbarger crystal

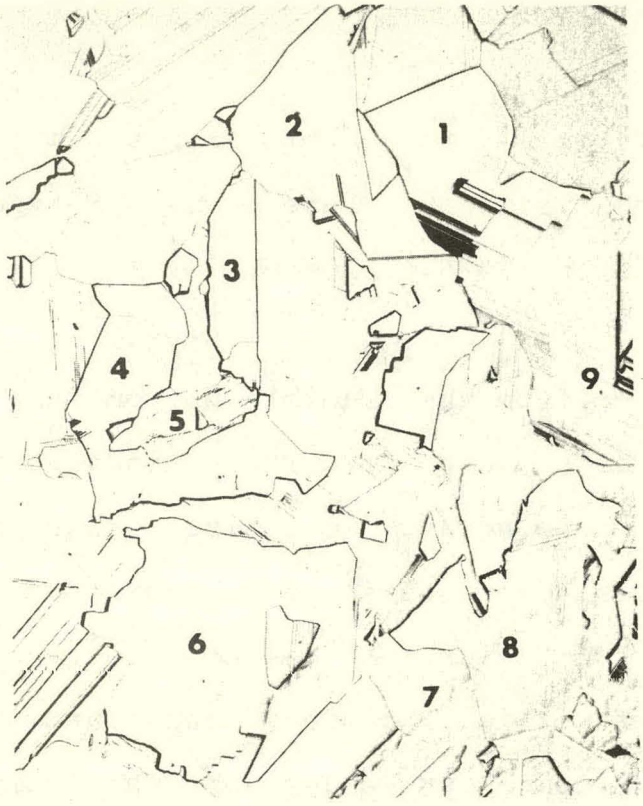

Fig. 6.

Grain Characteristics 2.5 cm from Crucible Bottom (10X)

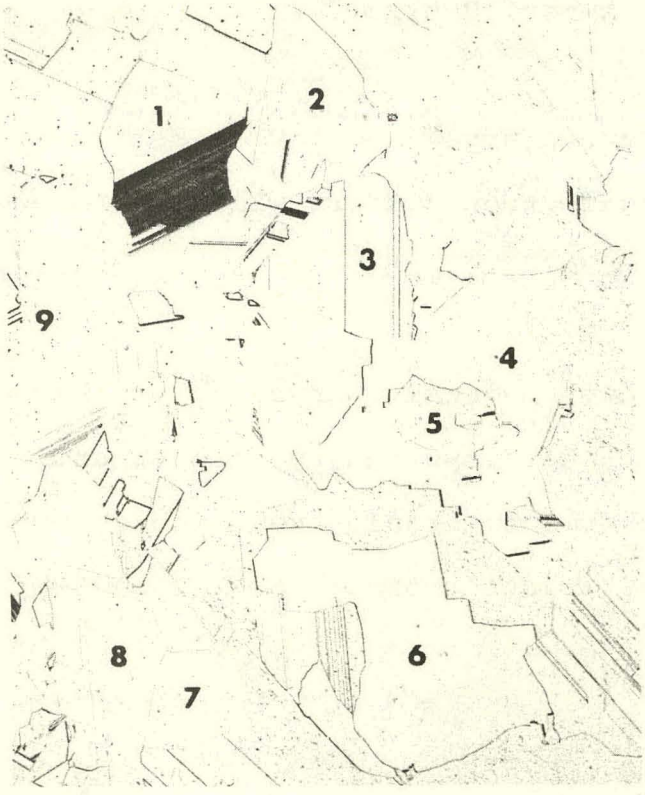

Fig. 7.

Opposite Side of 1.2 mm Thick Wafer Shown in Fig. 6. Grains Visible on Both Sides are Numbered.

growth is an effective simple technique used for many metals and alkali halides (6). The container should be inert and the material to be grown should contract upon freezing or at least not stick to the crucible walls. Silicon does neither and has not been successfully grown by this simple process. Recently (7), additional attempts have been made using the traditional fused quartz containters, and cracking of the ingot is a serious problem.

Silicon is capable of plastic deformation from the melting point (1415^{o}C) down to about 650^{o}C. Below that temperature, silicon responds to an increasing applied stress by deforming elastically until the fracture stress (cracking) is reached. In the temperature range 650^{o} to 20^{o}C, the thermal expansion coefficient monotonically decreases from 5 x $10^{-6}/^{o}$C to 2.4 x $10^{-6}/^{o}$C almost linearly. Thus, when silicon is solidified and then cooled below 650^{o}C in a quartz crucible, the silicon shrinks at a much lower rate than the crucible (the thermal expansion coefficient of fused quartz is 0.55 x $10^{-6}/^{o}$C in the temperature range 15-1000^{o}C). Since the silicon sticks to the quartz, cracking results as the silicon fracture stress is exceeded.

In 1972, it was shown that graphite is a durable substrate in contact with liquid silicon provided that the density is

greater than about 1.75 gm/cm^3 and the grain size is less than about 50 μm(2). The degree of carbon contamination of the silicon (about 20 ppm) is similar to the level of oxygen contamination when silicon is grown from conventional SiO_2 crucibles; however, unlike oxygen, carbon is not electrically active in silicon.

Graphites are available with a wide range of thermal expansion coefficients (1.1 to 8.3 X $10^{-6}/^{o}C$), some being isotropic and some anisotropic. To avoid cracking of the silicon charge and/or the crucible, the graphite or carbon crucible should have a thermal expansion coefficient in the range 650°C to about 20°C which either matches that of silicon or else, on the average, produces the same dimensional change.

The thermal expansion coefficient of vitreous carbon ranges from 3.5 x $10^{-6}/^{o}C$ at 650°C to 3.2 x $10^{-6}/^{o}C$ at 100°C and has about the same average dimensional change as silicon in this range (at 650°C, the silicon shrinks less than the carbon with decreasing temperature, while near room temperature, the silicon shrinks more than the carbon with decreasing temperature).

It is felt that grain size could be increased by seeding the initial growth at the bottom of the crucible.

Of course, any cross-sectional ingot shape - rectangular for example - could be produced by using an appropriate container shape.

The initial melt temperature and solidification rate used here were arbitrarily chosen and could probably be altered substantially.

3.2 Silicon Nitride

Wetting of silicon on CVD Si_3N_4 was tested. The CVD sample was a segment from a cylindrical crucible wall. The radius of curvature (in only one dimension) was 4 cm, and the segment thickness was 1.1 mm. The Si_3N_4 segment was degreased, etched in HF for 2 min., and rinsed. An etched silicon chip of 0.078 g weight was placed on the Si_3N_4 and heated to the silicon melting point under an argon ambient. The droplet was allowed to remain molten for several minutes and then was solidified. The droplet and substrate were then sectioned and etched to reveal the interface and contact angle. The entire section is shown in Fig. 8, and a close-up of one edge appears in Fig. 9. The observed contact angle (Fig. 9) is 23°. The partial wetting behavior indicates that capillary rise should occur with CVD Si_3N_4. This will be further investigated. While the main body of the droplet had the contact angle described above, a thin

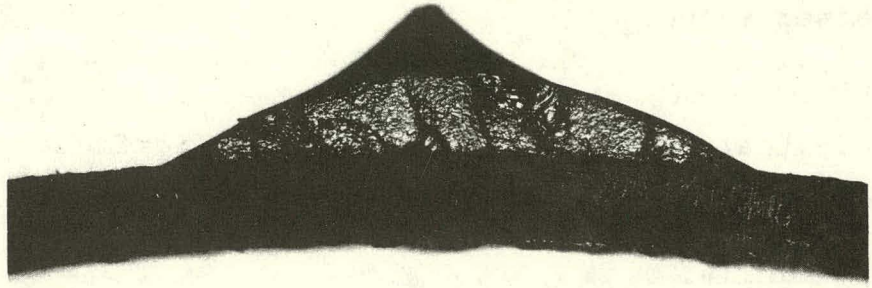

Fig. 8. Silicon Droplet Solidified on Si_3N_4-CVD Substrate (10X)

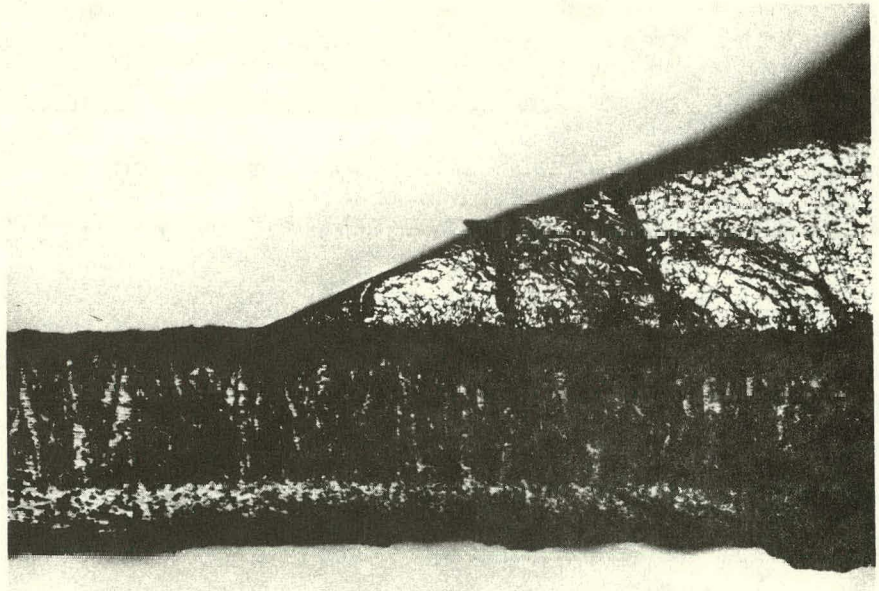

Fig. 9. Close-up (25X) of Left Edge of Droplet

film of silicon spread on the Si_3N_4 ahead of the main body. This is visible in Fig. 10, which is a top view of the droplet prior to sectioning.

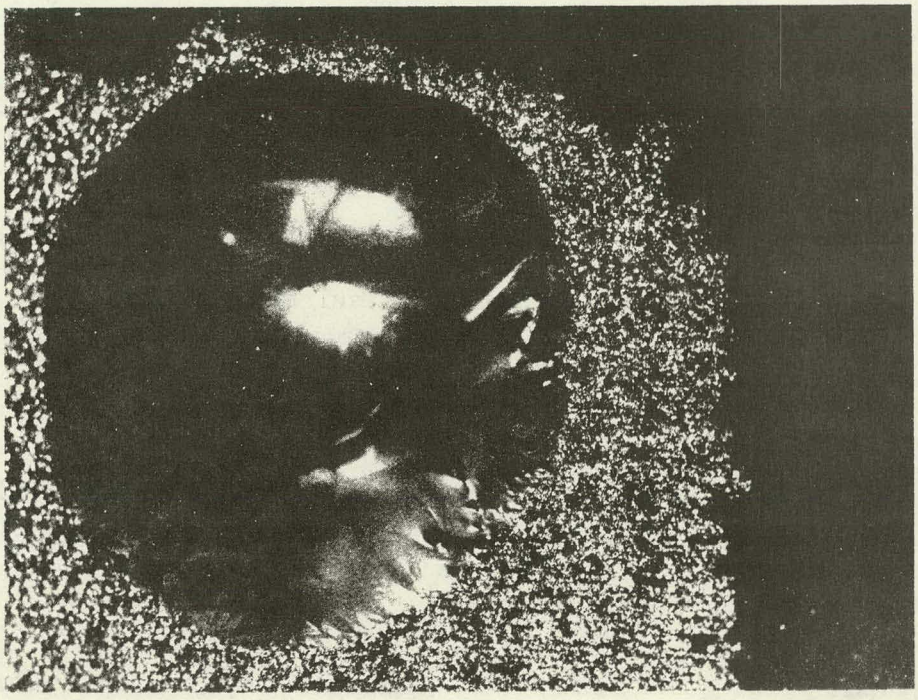

Fig. 10. Top View of Droplet (10X)

4.0 ACKNOWLEDGMENT

Technical assistance in performing the experiments discussed in this section was provided by F. Newman.

5.0 REFERENCES

1. H. E. LaBelle, Jr., Mater. Res. Bull. 6, 581 (1971).

2. T. F. Ciszek, Mater. Res. Bull. 7, 731 (1972).

3. T. F. Ciszek and G. H. Schwuttke, phys. status solidi (a) 27, 231 (1975).

4. J. C. Swartz, T. Surek, and B. Chalmers, J. Electron. Mater. 4, 255 (1975).

5. H. Fischer and W. Pschunder, IEEE 12th Photovoltaic Specialists Conference Record, 86 (1976).

6. S. L. Zerfoss, et al., "Crystal Growth at High Temperatures," Trans. Faraday Soc., 1949.

7. JPL LSSA Project Quarterly Report #2, pp. 4-76--4-77, Sept. 1976.

DIFFUSION LENGTH MEASUREMENTS BY SEM

by

R. G. Dessauer and E. W. Hearn

1.0 INTRODUCTION

The development of the method and equipment systems, here described in detail, is based on work done by Dr. R. N. Hezel for the characterization of silicon ribbon, (Ref. 1). Sample preparation methods for silicon wafers are included since they differ from those applicable to ribbons.

2.0 THEORY AND WORKING EQUATION

The diffusion length measurement is based on the expression:

$$I \sim e^{-x/L_n} \qquad \text{eq. 1} \qquad (1).$$

where:

I = current at junction edge due to electron beam induced current (see Ref. 1, Fig. 12).

x = Distance from e-beam impact point to junction edge.

L_n = Diffusion length.

This expression can be transformed to give diffusion length as a function of measured distance:

$$L_n = \text{Log } e\ (\Delta x) \qquad \text{eq. 2 (see Appendix I).}$$

The distance (Δx), measured along the x-axis of any log I vs. x plot is that which is subtended from the straight portion of the curve by one decade of (log) current.

Taking into consideration the x-y recorder pen travel and electron beam scanning rates, and substituting $\frac{D}{m}$ for Δx in eq. 2, the working equation becomes:

$$L_n = \frac{(10^4 \log e)(\ell)(^{R}s)D}{(t)\qquad (M)(m)} \quad \mu m \qquad \text{eq. 3}$$

where, 10^4 is the conversion from cm. measurements to μm

and, ℓ = length of scan measured on screen of SEM cathode ray tube (cm).

R_s = X-Y recorder pen sweep rate (in X direction) (sec/cm).

D = X-Y recorder pen excursion (in Y direction) for one decade of log current applied (cm).*

t = Time per one scan of length ℓ (sec).

M = SEM magnification (dimensionless)

m = Slope of straight sections of log I vs. x curve.

*D is chosen from Table I. It depends solely on the log converter output scale factor and the X-Y recorder Y - range settings (see Appendix 2).

A simple aid was devised to facilitate reading the slopes of log I vs. x curves produced on the recorder. It consists of a transparency showing slope values on a vertical (y) axis and a distance of unity on the same scale laid out along the x-axis, (see Fig. 1). The transparent overlay over the straight section of the log I vs. x curve directly on the recorder chart paper. Its axes are arranged parallel to those of the chart, and the end point of the x distance is placed on the lower portion of the straight section. The slope may then be read off the scale directly at the point of intersection of the Y-axis with the upper portion of the curve. The overlay may be reversed for slopes having

TABLE I. "Height" (D) in cm. on recorder chart (i. e., pen excursion in Y-direction) for input change of one decade of log current with available combinations of log converter output scale factor and recorder Y-range, (see Appendix 2).

Log-Converter Output Scale Factor	Recorder Y-Range (mv./cm.)	Y-Scale Reduction	Height One Decade (D) cm.
5	.25	1	161.4
5	.5	1/2	80.7
10	.25		
10	.5	1/4	40.4
20	.25		
20	.5	1/8	20.2
5	2.5	1/10	16.1
5	5	1/20	8.1
10	2.5		
10	5	1/40	4
20	2.5		
20	5	1/80	2

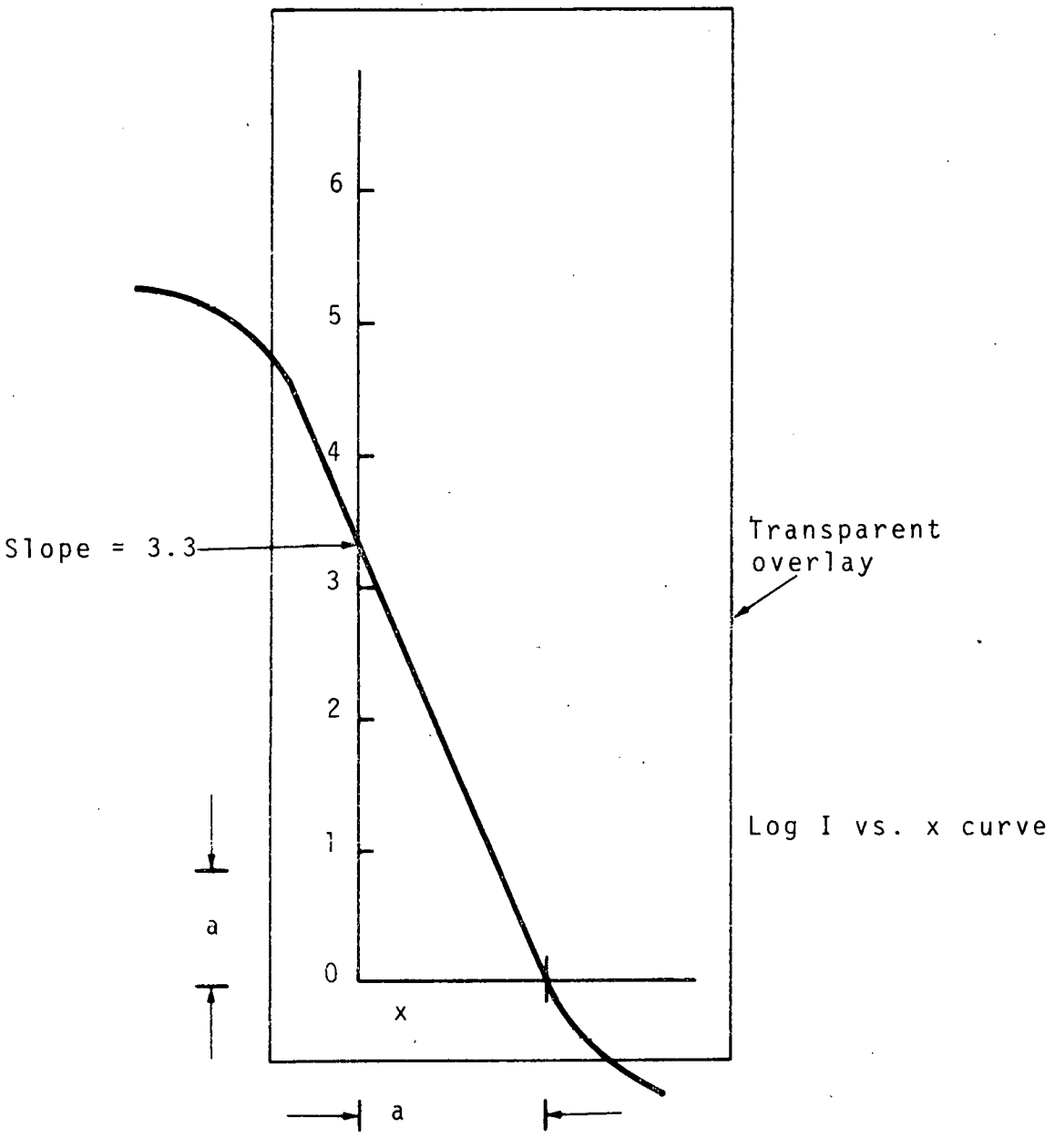

Distance "a" is arbitrarily chosen. (When a is 2.5 cm the scale will fit most curves obtained with the described equipment).

Fig. 1 Slope Measuring Aid

opposite sign due to reversing of scan direction. A maximum slope value of 6 was found adequate for the described equipment.

3.0 EQUIPMENT AND OPERATION

The SEM (Cambridge S-4) is operated in reflective and electron beam induced current (EBIC) mode for alignment of diode areas to be used for measurement. The diffusion length measurement, i.e., the recording of the log I vs. x curve, is done with a line scan of the e-beam under the control of a Princeton GammaTech. Model 303 display and scan generator in conjunction with a PGT Comparascope II Multi-Channel Analyzer.

The EBIC from each of up to four test diodes in turn (see Ref. 2 for description of 4-probe sample stage) is fed through the control unit and SEM-SCA to a Model HP7561A logarithmic converter (see Fig. 2). The converted current signal is fed to a Model HP 7045A X-Y recorder. (Note: see Ref 2 - Fig. 4 for schematic diagram of control unit).

4.0 SAMPLE PREPARATION

4.1 Polished Wafers

Schottky barriers cannot be used with polished wafers,

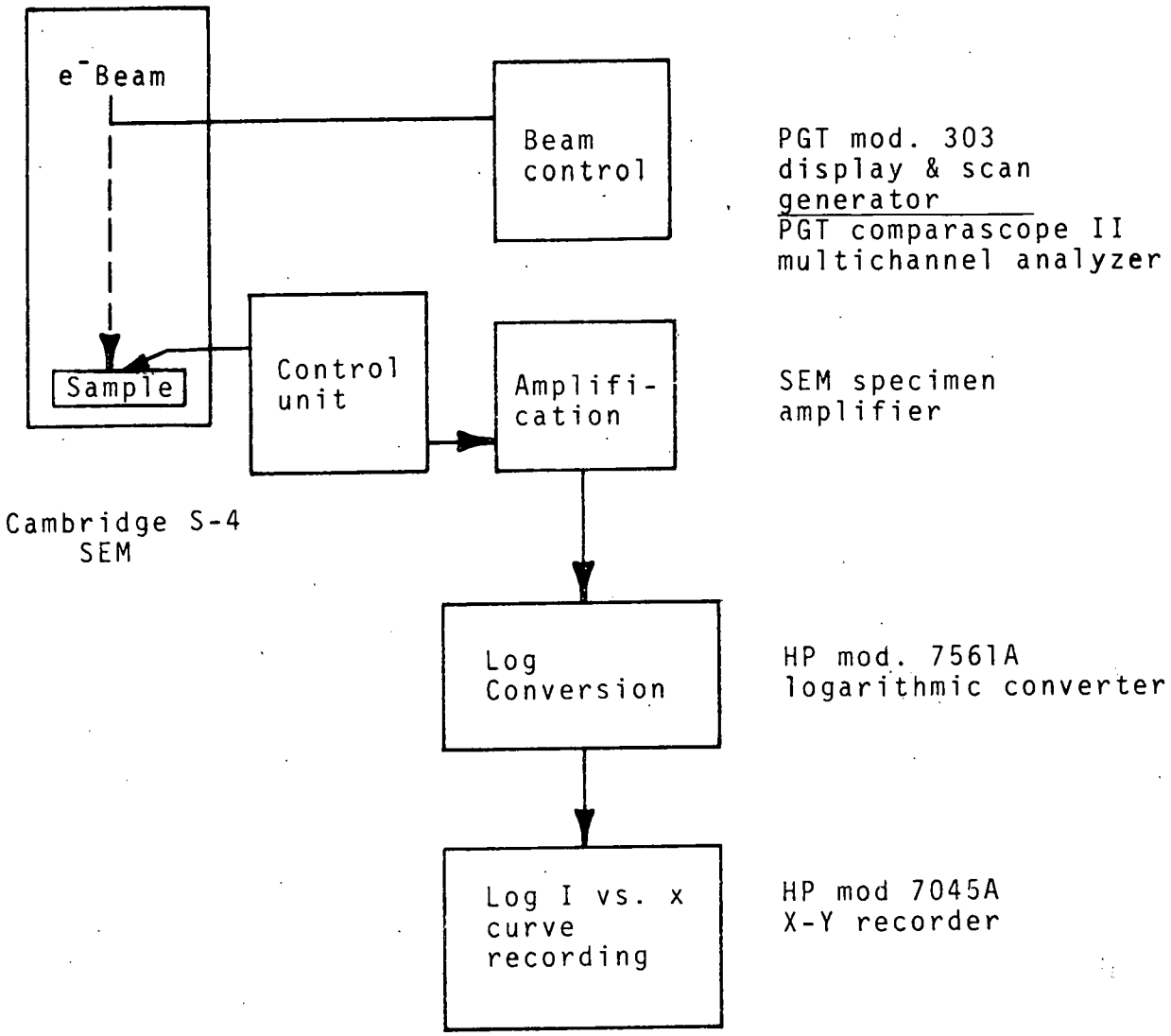

Fig. 2: Diffusion length measurement
current flow and equipment chart

since they result in excessive noise and repeatability problems. This may be due to the large area diodes required for diffusion length measurements. Therefore, diffused junctions are used. If diodes diffused through oxide masking cannot be obtained, mesas may be etched on blanket diffusions. The mesas are then cleaved, and diffusion length measurements are made on the cleaved surfaces. Etched mesas alone cannot be used for diffusion length measurements due to perimeter and surface etching effects. However, the mesas are useful in conjunction with cleaving where they prevent junction shorting. The vertical junctions obtained in this way provide the additional advantage of constant distance to electron impact area regardless of penetration depth.

4.2 Silicon Ribbon

Schottky barriers are preferred for diffusion length measurements on silicon ribbon. Barriers produced with $\approx$ 2000 Å of evaporated aluminum give satisfactory results. This may be due to surface roughness and/or carbon deposits on ribbon surfaces.

The cleaved mesa technique presents some difficulty

when used with ribbons. The often closely spaced boundary and defect lines in ribbons are not discernable when the sample is in measurement position (edge view). This can cause loss of area identification.

5.0 EQUIPMENT SET-UP

The logarithmic converter and X-Y recorder are connected as shown in Fig. 3. The 20.4 KΩ resistor across the recorder input terminals is required for impedance matching (see Ref. 3). Figure 3 shows the polarity for a Schottky diode on P-type material. As stated earlier, Schottky barriers are preferred for ribbons, while diffused junctions are used for wafers.

5.1. Scanning Electron Microscope (SEM)

The SEM is set up for EBIC mode with condenser lens current as follows:

Lens #1 : .54 a,

Lens #2 : .22 a.

5.1.1 Beam Control Equipment

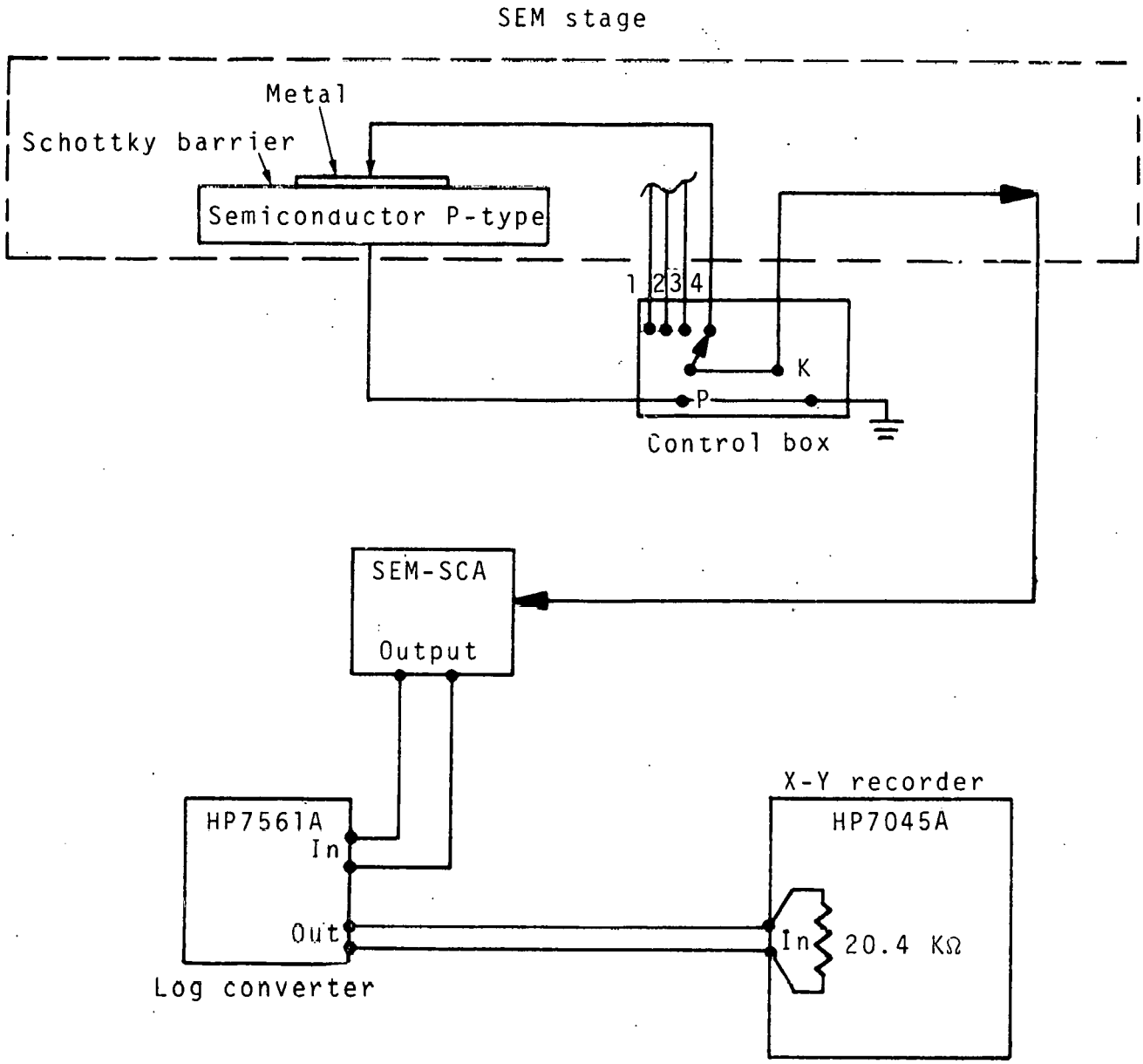

Fig. 3: Equipment connections

5.1.2 Multi-Channel Analyzer (MCA)

1. The cycle switch (in rear) is set to "RE-CURRENT" to prevent damage to the CRT by a stationary beam at the end of a scan. Note: This switch affects the scan time setting (as will be discussed under "scan time" in the section on operating procedures).

2. In the MCA Program section, the Spectrum/ Time Scan switch is switched down to "Time Scan." All other program switches should be in the UP position.

3. MCA power is switched on, and three minutes allowed for warm-up.

5.1.3 Display & Scan Generator (DSG)

1. The scan direction is set by the "X" switch (+ or -) in rear of the DSG. This allows scanning toward or away from the junction as desired.

2. The DSG Function Switches are set as follows:

#1 on "SCAN"

#2 on "LINE"

#3 on "DSG"

3. A scan length of 2 cm (on CRT screen) has been found adequate for all diffusion lengths encountered. This value is obtained when the "X expand" pot is set at 1.0. Other lengths may be obtained, if required, by varying the setting.

6.0 SAMPLE SET-UP

Samples are placed on the SEM stage at 0° tilt, (horizontal)

It is preferable to scan perpendicularly to the edge of a square or rectangular junction area, or radially if a circular diode is used. Thus, the scan path will lie along the shortest distance from e-beam impact point to junction area edge. The generated electrons, which travel to the collecting field by the shortest path, will thus travel along the scan path, resulting in a well-defined straight section of the log I vs. x curve.

7.0 OPERATING PROCEDURES

The selected diode is connected on the control unit to the SCA. It is observed in normal EBIC mode and aligned for scanning at low magnification (50 x for a 60 mil dia. diode). The diode may be outlined on the CRT screen with a grease pencil to mark its position when the image disappears upon switching to line scan mode.

The SEM is placed in line scan mode by setting the scan generator as follows:

a. switch "Visual Raster" to "EXT."

b. Switch "Vert./Hor." to "EXT."

The EBIC image will disappear and a spot image will mark the beam location. The intensity on both CRT's may have to be turned down to avoid burning them. The MCA "Stop" button should be depressed to stop scanning and allow placement of the beam at the desired scan location. (Pushing the "stop" button returns the beam to scan start position). To place the beam, the spot is moved by two pots on the DSG:

Y direction: "Scan Position" Pot

X direction: "X OFFSET" Pot

After the beam has been moved to the desired scan location with the "Scan Position Pot.," to first move the spot outside the junction area (as marked on CRT screen) with the "X OFFSET" pot, it is then moved slowly toward the area until the "INPUT LEVEL" meter on the log converter shows a maximum in the "operate" region. This indicates that the junction edge has been reached. It is desirable to leave the beam at the starting point for 10-20 seconds before starting the scan to allow the area to reach equilibrium conditions.

The scan is started by depressing the MCA start button. Simultaneously, the recorder pen is started to record the log I vs. x curve. The slope of the curve should lie between 1 and 6, and the straight section should be as long as possible for measurement ease and accuracy. Since the EBIC level varies for different samples, the SCA current range and the following five parameters have to be adjusted to obtain the desired curve. (Note: see Table II for SCA amplification).

7.1 Scan Speed Adjustment

The time for beam travel over the previously chosen scan length is set on the MCA. When the scan has been

TABLE II. Specimen Current Amplification By SCA of Cambridge S-4 Scanning Electron Microscope

CURRENT RANGE SWITCH SETTING	AMPLIFICATION		INPUT SPECIMEN CURRENT RANGES FOR CURRENT RANGE FACTOR METER READINGS	
	A_s (X)	Log A_s	MIN. (OUTPUT .1 MA.)	MAX. (OUTPUT 1 MA)
10^{-12}	10^8	8	10^{-12}	10^{-11}
10^{-11}	10^7	7	10^{-11}	10^{-10}
10^{-10}	10^6	6	10^{-10}	10^{-9}
10^{-9}	10^5	5	10^{-9}	10^{-8}
10^{-8}	10^4	4	10^{-8}	10^{-7}
10^{-7}	10^3	3	10^{-7}	10^{-6}
10^{-6}	10^2	2	10^{-6}	10^{-5}
10^{-5}	10^1	1	10^{-5}	10^{-4}
10^{-4}	10^0	0	10^{-4}	10^{-3}

set for "RECURRENT" (switch at rear of MCA) a setting of 1 on the "PRESET SEC/COUNT" dial gives a scan time of 1000 seconds, (10^{-1} = 100 seconds, etc.). The "MULTIPLIER" switch gives multiples of these values as indicated. (Note: When the switch is in "single" scan position the time values are doubled, i.e., 1 = 2000 seconds, etc.).

The scan speed affects the slope of the curve.

7.1.1 Log Converter: Input Attenuation

The input attenuation affects the vertical location of the curve on the recorder chart. To move the curve up on the chart, the input attenuation is reduced, and vice versa.

7.1.2 Log Converter: Output Scale Factor

The output scale factor affects the Y-scale of the curve. Lower values expand the curve, higher values reduce the Y-scale. Consequently, this parameter affects the decade height (D) used in the diffusion length calculation, (see Table I).

7.1.3 Recorder: Y-Range

The X-Y recorder Y-range also affects the Y-expansion of the curve and thus the height (D) of a decade of current, (see Table I).

7.1.4 Recorder: Sweep Rate (Time Base X)

The X-Y recorder sweep rate affects the slope of the log I vs. x curve.

The scan is complete when the current has levelled off to background value at the low end of the curve (if the scan is away from junction area). When the scan is made toward the collecting field, the end current will level off to the full EBIC value in the diode area. Upon completion of the scan, the recorder is switched to "RESET" to lift and return the recording pen. The "Stop" button on the MCA is then depressed to stop the scan and return the beam to the starting position.

8.0 RESULTS

Subsequent scans, made over the same path, result in lower overall current levels. This is due to a charging effect in

the material (see Ref. 4).

In general, diffusion length values for materials measured fell between 4 and 40 μm. Epitaxial layers were at the low end of this scale. Values measured in known defect areas on ribbons were usually 10-30% lower than those measured in the surrounding good material.

9.0 CONCLUSION

The system described provides a relatively simple and rapid means for diffusion length measurements on semiconductor material. The collecting fields may be provided by either diffused junctions or Schottky barriers.

The results cannot always be correlated with those obtained with other diffusion length measurement techniques for the same material. However, the method is useful for evaluating material through relative values of diffusion length.

10.0 REFERENCES

1. Lifetime Characterization of Silicon Ribbons, by G. H. Schwuttke, K. H. Yang and R. Hezel, JPL Contract No. 954144, Silicon Ribbon Growth by A Capillary Action Shaping Technique, G. H. Schwuttke, Principal Investigator, Technical Progress Report No. 5, 9/15/76.

2. Equipment and Procedure for Defect Display under MOS Structures in Silicon Ribbon for Lifetime Interpretation, by R. G. Dessauer and E. W. Hearn.

3. Operating and Service Manual HP7561A Logarithmic Converter, Hewlett Packard, Moseley Division, or...

   Operating and Service Manual 60D/60DM Logarithmic Converters, Hewlett Package, Moseley Division.

4. Contrast Mechanisms in Electron Beam Images of Interface Structures, W. R. Bottoms et al, J. Vac. Sci. Technol., Vol. 12, No. 1, Jan./Feb., 1975.

THIS PAGE

WAS INTENTIONALLY

LEFT BLANK

APPENDIX

1. Derivation of diffusion length measurement equation (eq. 2) from theoretical expression (eq. 1).

Given $I \sim e^{-x/L_n}$ eq. 1

taking log of both sides:

$$\log I = - \frac{x}{L_n} (\log e)$$

or $\log I = - (\frac{\log e}{L_n}) x$, which is in the form of the straight line equation:

$$y = mx$$

where $y = - \frac{\log e}{L_n}$ = slope of the straight line

let y = one decade of log current (see App., Fig. 1)

then $\log 10^{-a} - \log 10^{-(a+1)} = (\frac{\log e}{L_n}) (x_2 - x_1)$

or $- a + (a+1) = (\frac{\log e}{L_n}) \Delta x = 1$

and $L_n = (\log e) \Delta x$ eq. 2

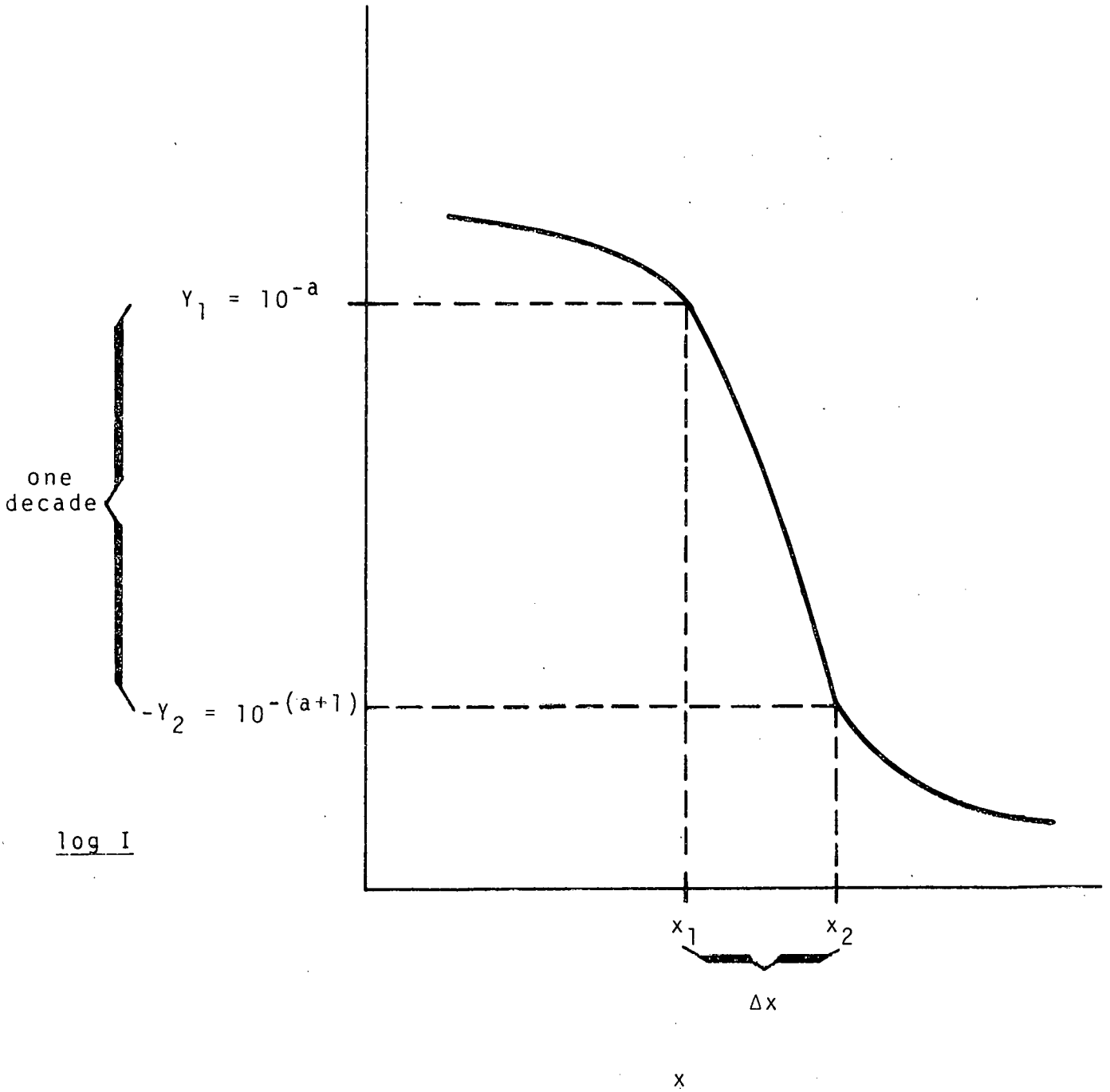

Appendix Fig. 1: Log current vs. distance from e-beam impact point to collecting junction for derivation of diffusion length measurement equation.

2. A Mathematical Relationship Between Sample Current and Recorder Pen Travel in the Y-Direction - Includes a Derivation of "D" (recorder pen Y-excursion for input change of one decade of log current.

a. Log Converter Signal Processing

The instrument has an output of 60 mv. for a one volt input with zero attenuation and an output scale factor of 10 db/in. (Ref. 4). (For a 1 mv. input the output will be almost zero.) The basic input range is 1 mv. to 1 volt, with a corresponding linear output range from slightly greater than zero to 60 mv. The instrument's input ratio is thus 1000/1.

The basic equation for expressing power levels by voltage ratios is:

$$\text{decibels (db)} = 20 \log {}^{E_2}/_{E_1} \qquad \text{eq. 1}$$

Substituting the instrument input ratio in eq. 1:

$$\text{db} = 20 \log \frac{1000}{1} = 60 \qquad \text{eq. 2}$$

(The basic range is thus 60 db).

It follows that the output of the instrument is proportional to the logarithm of the input (since the output for a 1000 mv. input is 60 mv) thus:

$$\text{output} = 20 \log \text{input}$$

$$\text{or} \quad \log \text{input} = \frac{\text{output}}{20}$$

(with zero attenuation and an output scale factor of 10 db/in).

Input attenuation settings other than zero will affect the output according to a general equation (eq. 4) derived as follows:

from eq. 1 : $\frac{E_2}{E_1} = 10^{.05N}$ where N = db.

thus: $\log \frac{\text{input}}{10^{.05N}} = \frac{\text{output}}{20}$ eq. 3.

where N is the input attenuation setting in db.

or $\log \text{input} = \frac{\text{output}}{20} + .05N$ eq. 4.

The output divisor (20 in eq. 4) is related to the output scale factor as follows:

$$\text{output divisor} = 200\ (\text{Scale Factor})^{-1} \qquad \text{eq. 5.}$$

Thus, with output scale factor 5 of db/in., for example:

$$\log \text{ input} = \frac{\text{output}}{40} + .05N$$

The general expression describing log converter signal processing can thus be written:

$$\log V_i = (5 \times 10^{-3} F)\, V_o + 5 \times 10^{-2} N \qquad \text{eq. 6}$$

which reduces to:

$$\log V_i = 5 \times 10^{-2} (.1FV_o + N)$$

where V_i = input voltage in mv.

V_o = output voltage in mv.

F = output scale factor (db/in.)

N = input attenuation (db)

b. Relationship Between Sample Current and Recorder Pen Y-Excursion

The general expression for log converter signal

processing (eq. 6, part a.) for convenience, may be written:

$$\log V_i = aV_o + b \qquad \text{eq. 1.}$$

where a and b are constants determined by the log converter settings. Ohm's low is applied to obtain log input in terms of current since log current is the ordinate of the log I vs. x plot whose slope determines diffusion length.

let R_i = log converter input impedance in ohms

i = input current in ma

then: $\log i = \log \left(\frac{V_i}{R_i}\right) = \log V_i - \log R_i$

substituting from eq. 1:

$$\log i = a V_o + b - \log R_i \qquad \text{eq. 2.}$$

Note: The input impedance given in Ref. 4 is $\tilde{}$ 2 meg. Ω. It was checked by electrometer and found to vary from 2×10^6 Ω to 2.2×10^6 Ω depending on input attenuation setting. Log R_i thus varies from

6.301 to 6.342. A rounded value of log R_i = 6.3 represents an error of less than 2%.

The log converter input current (i) in eq. 2 is the EBIC from the sample as amplified by the SCA.

$$\therefore \log i = \log (i_s A_s)$$

Where i_s = EBIC from sample

A_s = Amplification factor of SCA (given in Table II.

It follows that:

$$\log i = \log i_s + \log A_s$$

Thus, the ordinate of a "log I vs. x" curve (where $I = i_s$) is:

$$\log i_s = \log i - \log A_s \qquad \text{eq. 3}$$

Note: The values for log A_s, are digital, vary from 0 to 8 and are given in Table II.

Substituting eq. 2 in eq. 3:

$$\log i_s = aV_o + b - \log R_i - \log A_s \quad \text{(ma)}$$

$$= a\,(R_y)(Y_r) + b - \log R_i - \log A_s$$

where R_y = Recorder Y-range setting mv./in.

Y_r = Pen Displacement on Y axis (inches)

Thus: $Y_r = (aR_y)^{-1}(\log i_s - b + \log R_i + \log A_s)$ eq. 4.

c. Derivation of "D" (Recorder Pen Displacement for an Input Change of One Decade of Log Current)

The relationship between recorder pen displacement (Y_r) and sample EBIC (i_s) is given by eq. 4, part b. The change in recorder pen displacement due to a change of sample EBIC follows:

$$\Delta Y_r = (aR_y)^{-1}\left[(\log i_{s_1} - b + \log R_i + \log A_s) - (\log i_{s_2} - b + \log R_i + \log A_s)\right]$$

$$= (aR_y)^{-1}(\log i_{s_1} - \log i_{s_2})$$

or $\Delta Y_r = (aR_y)^{-1}(\Delta \log i_s)$ eq. 1.

The desired value "D" is ΔY_r as shown in eq. 1 for ($\Delta \log i_s$) equal to one decade. In Appendix Section 1, it was shown that one decade of log current is equal

to unity.

$$\therefore D = (aR_y)^{-1} \qquad \text{eq. 2.}$$

Thus, equation 2 shows that the required value "D", as given in Table I, depends only on the recorder Y-range setting (R_y) and the log converter output scale factor (F) in the relationship $a = 5 \times 10^{-3}F$. Note: If R_y is in mv./cm., D will be in cm. (Eq. 2 has been fully supported by experimental data).

Note that the units of the quantities on each side of eq. 2 do not agree. "D", of course, is measured in units of length, and eq. 2 does give the correct values. The disagreement of units is due to the combined use of Ohm's law and logarithms. When this is done, the meaning of units is lost, but the numerical results will be correct. Section d gives an explanation of this.

d. Effect of Logarithms on Ohm's Law

OHM'S LAW IN STANDARD TERMS	OHM'S LAW IN LOGARITHMIC TERMS
V(volts)=I(amps)xR(Ω)	logV("log volts")=logI("log amps") +logR("log ohms")
$V = IR$	$\log V = \log IR = \log I + \log R$
$I = \frac{V}{R}$	$\log I = \log\frac{V}{R} = \log V - \log R$

Therefore:

Unit-wise:

Volts and "log volts" can be "handled mathematically" with each other, i.e., they can be divided/multiplied by each other, or added to and substracted from each other, and the result will have the units of volts.

The same applies to "log amps" and amps - the results will have the units of amps.

It also applies to "log ohms" and ohms, where the results will be in ohms.

but:

Volts cannot be handled with log amps or log ohms,
Amps cannot be handled with log volts or log ohms,
Ohms cannot be handled with log volts or log amps,

i.e., V(volts) $\neq$ log I(log amps) x R(ohms) etc...

During the transformation from Y_r to ΔY_r (eq. 1

part c, to eq. 4 part b), several numerical quantities were cancelled. This could not be done if units were to be preserved. The numerical results for eq. 1, part c, however, are correct. Note that the units on both sides of eq. 4, part b, do agree and are units of length. Log i_s, in that equation, is in units of log amps, log R_i in units of log ohms and R_y in units of volts per unit length. The quantities a, b and A_s have the effect of dimensionless constants and need not be considered. It follows that since log amps + log ohms = log volts, OR volts the units of this equation (part b, eq. 4) agree and are units of length.

THIS PAGE

WAS INTENTIONALLY

LEFT BLANK

EQUIPMENT & PROCEDURE FOR DEFECT DISPLAY UNDER MOS STRUCTURE IN SILICON RIBBON FOR LIFETIME INTERPRETATION

by

R. G. Dessauer and E. W. Hearn

1.0 INTRODUCTION

Investigations have shown that twin and grain boundaries and associated dislocations in silicon ribbon degrade life time, (Ref. 1). In this previous work, lifetime in areas containing such defects was measured by means of circular MOS capacitors. It is desirable to investigate the electrical activity of the various defects under these capacitors so that their individual effect on life time can be more closely established.

Subsurface defects in semiconductor structures are routinely displayed by a scanning electron microscope (SEM) in EBIC mode. The structures must contain collection fields such as are due to diffused junctions or Schottky barriers. The various defects act as recombination centers, locally reducing EBIC and thus providing contrast for their display.

The intensity of contrast is taken as a measure of their electrical acitivity.

MOS structures may be similarly examined in EBIC mode if conduction through the oxide is obtained. A technique for this (Ref. 2) is applied to 5 mm dots such as described in Ref. 1. The previously-measured lifetime value corresponding to each capacitor can then be correlated with the total electrical activity of defect lines within each dot. The relative electrical activity of the various types of defects, identified subsequently by etching, light optical, and transmission electron microscopy may be evaluated by correlation with the EBIC micrographs, (Ref. 3).

2.0 EXPERIMENTAL

2.1 Sample Preparation & Description

The ribbon material, MOS process, capacitor lay-out and dot size are fully described in Ref. 1, (pp. 2-3). The samples are cut square, approximately 9.5 mm per side to fit the four-probe SEM sub-stage described later. The two resulting dot patterns permit full utilization of the sub-stage probes. The patterns are shown in Fig. 4.

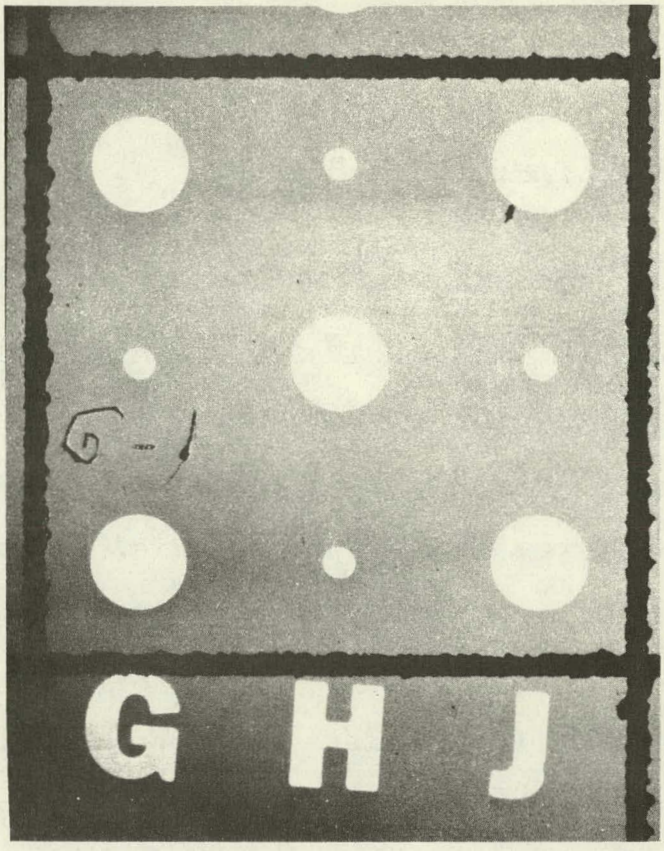

Wafer #311-3

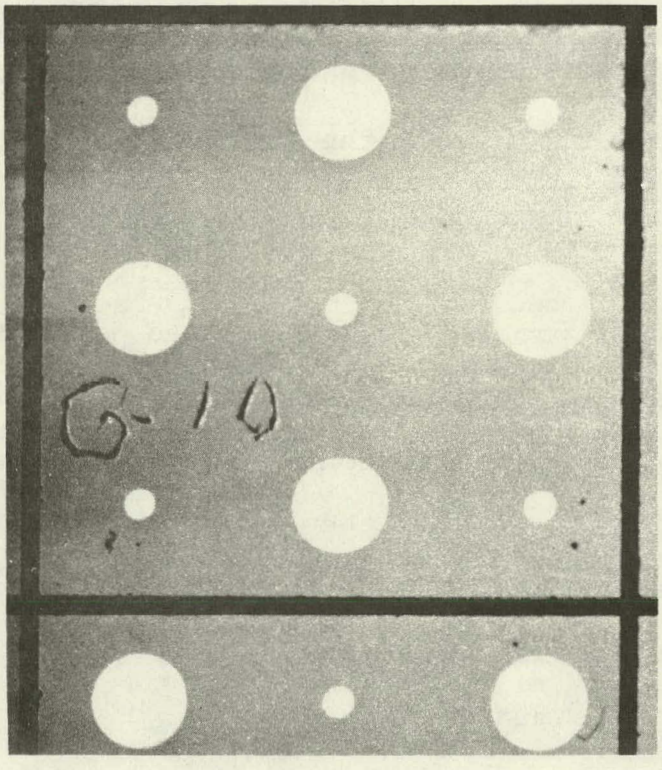

Wafer #312-4

Fig. 4. MOS Dot Pattern for SEM EBIC Mode Testing

2.2 Equipment & Instrumentation

The scanning electron microscope used in this work is a Cambridge-Imanco Model S-4 with a Series 200 micro-analysis sample stage. The stage has been adapted to accept a specially designed 4-probe sub-stage. A close-up view of the substage Fig. 5a is seen installed on the Series 200 sample stage in Fig. 5.

The sub-stage consists of four movable probe holders mounted within the periphery of the stage body.

Bias thermal stressing (BTS, Ref. 2) is applied to the samples at -20V and 300^{o}C for 20 minutes. The samples are cooled to 50^{o}C the stressing voltage, and examined at room temperature.

The four probe pins are clamped in slotted brass balls by means of retaining screws, one of which serves as an electrical connection. The pins may be coarsely positioned within the brass balls. The balls are mounted in sockets electrically isolated from the probe holder bases. The probe holder mechanism provides the fine adjustment.

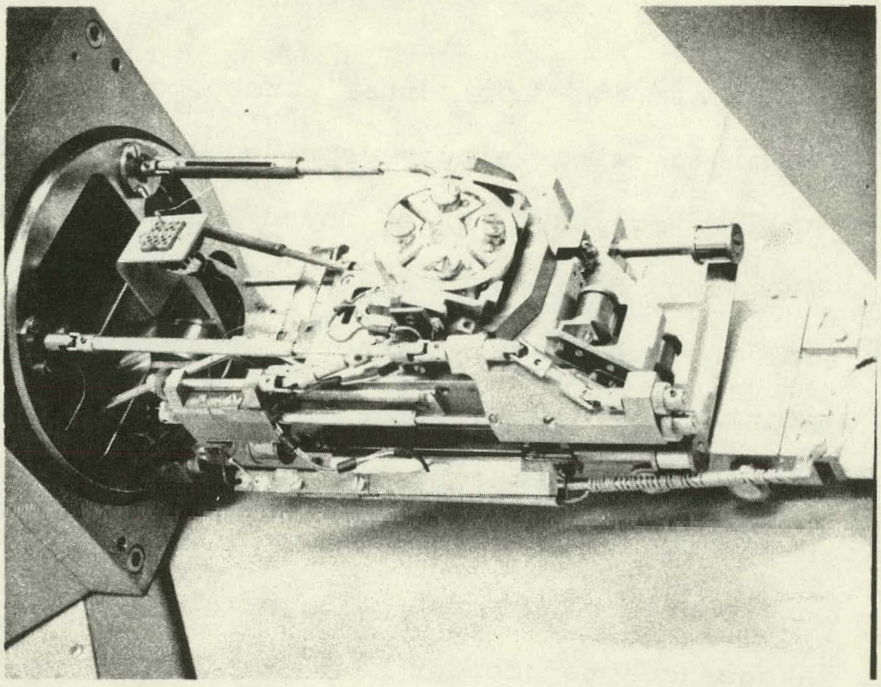

Fig. 5. SEM-EBIC Substage in Place on Series 200 Sample Stage

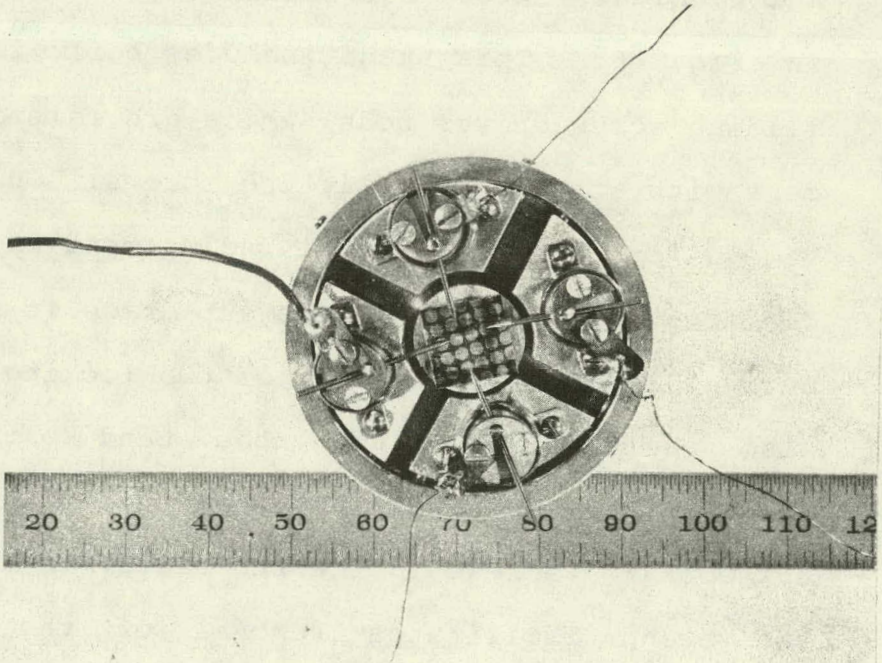

Fig. 5a. SEM Substage for MOS EBIC Mode Testing

Vertical and horizontal probe position adjustment is obtained with single spring loading of each probe holder against three round-nosed adjustment screws. The two horizontal (X-Y) alignment screws are located in the sub-stage periphery. They also serve as swivel points for the vertical movement as the lifting screw bears against the bottom of the probe holder. Contact pressure to the sample may be adjusted by varying the angle of the probe pins prior to clamping. The sub-stage accepts standard 1.27 cm SEM sample stubs and includes a stub clamping screw.

A convenient fixture for loading the sub-stage is shown in Fig. 6. This stand includes built-in, vertically sliding screw driver rods, which are raised for engagement with the probe lifting screws. Guides are provided for the horizontal adjustment and sample stub clamping screw drivers. The sub-stage is held in place during loading by means of two locking rods. These also position it within the stand so that all screw drivers and guides in the stand are aligned with the appropriate screws in the sub-stage. A lifting pin in the stand facilitates removal of the sub-stage. A contact screw and electrical jacks provide for

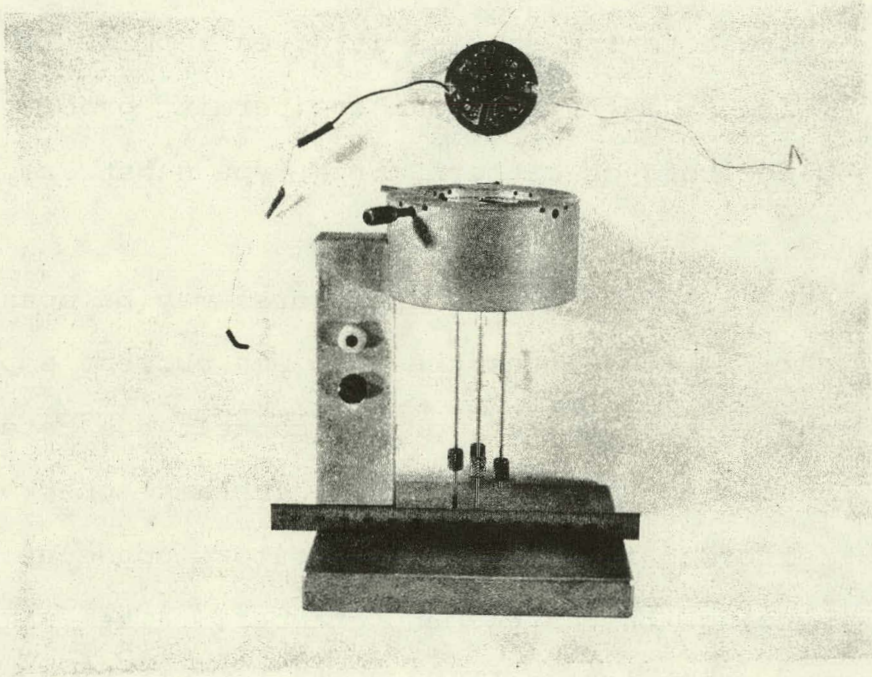

Fig. 6. Substage Loading Fixture

connection of a capacitance meter (Boonton Electronics Corp. Model 71A-R) to assure proper probe contact.

A schematic of the circuit used to apply reverse bias voltage to the samples is given in Fig. 7. A reversing switch is provided to permit processing of MOS capacitors on either P or N type substrates.

Each of four MOS capacitors may be connected alternately to either the specimen current amplifier (SCA) and voltage source, or the capacitance meter. Display, recording and probe pin contact check may thus be performed for all four capacitors consecutively without opening the specimen chamber. The sample may be grounded without bias voltage by turning the bias control to zero.

2.3 Procedure

The sample is installed and probe pin contact is checked with the capacitance meter. The SEM is set up for specimen current mode. Condenser lens current values used are .55 and .22 amps for lenses No. 1 and No. 2, respectively, with full collector voltage. An accelerating voltage of 30 KV is used to penetrate the metal and oxide layer.

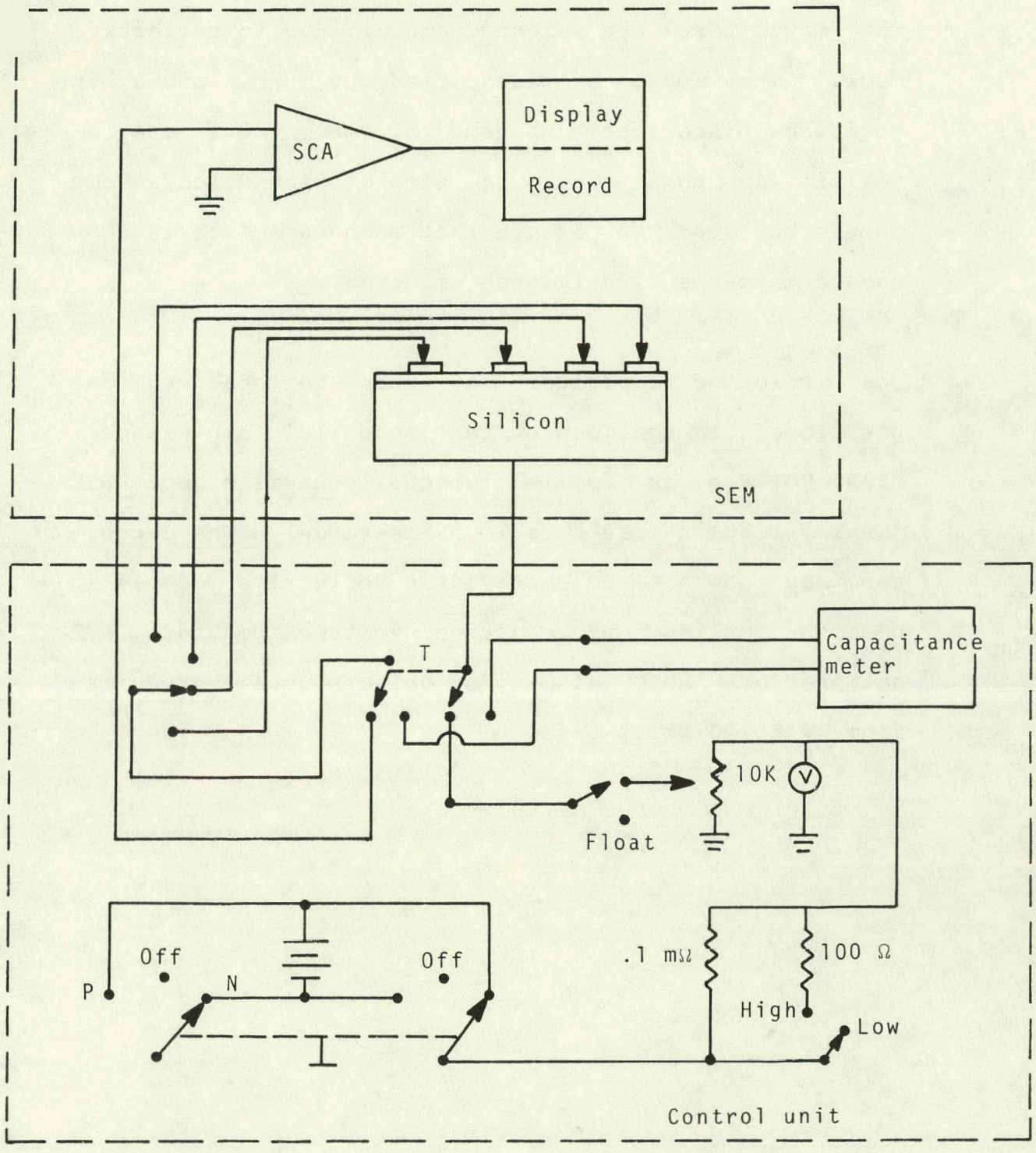

Fig. 7. Reverse bias voltage application circuit

The capacitors are selected and aligned in reflective mode. They must be identified by their probe pin positions since the unbiased aluminum dots are invisible in this mode. A sample orientation scheme should be used to assure that each capacitor is connected into the circuit when selected.

The selected capacitor may then be observed and positioned in specimen current mode (10^{-9} amp. range). Bias voltage is applied gradually until a good EBIC display results (10^{-6} to 10^{-4} amp range). The capacitor may now also be observed in reflective mode as it becomes outlined by negative voltage contrast. A satisfactory EBIC display of defects usually requires from 10 to 40 volts bias.

3.0 RESULTS & DISCUSSION

A good EBIC micrograph is shown in Fig. 8. Defect lines and bands of varying contrast, indicating relative electrical activity are seen crossing the MOS capacitor.

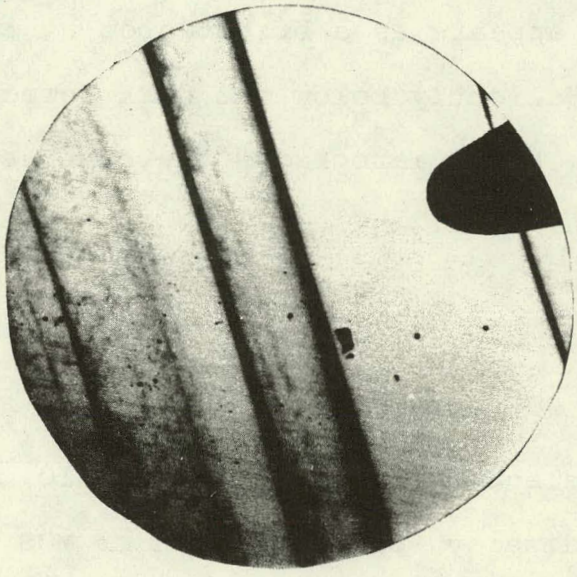

Fig. 8. SEM EBIC Micrograph of MOS Capacitor on Silicon Ribbon

In some cases an EBIC display is not obtained until localized breakdown of the oxide occurs, usually at a bias in excess of 50 volts. After breakdown, EBIC displays are

obtained at normal bias voltages (40V). However, a sharp change of contrast occurs at the breakdown point. The point itself appears as a bright spot due to the high current at this location. This is illustrated in Fig. 9, which shows two views of the same capacitor scanned vertically (A. top to bottom) and horizontally (B. left to right). The breakdown point appears as a bright spot at the left side of the capacitor slightly below the dark defect line. It can be seen that in both micrographs the contrast change occurs at the breakdown point.

4.0 SUMMARY

The scanning electron microscope in EBIC mode is a useful tool for the display of defects under MOS capacitors previously treated with Bias Thermal Stressing.

A feature of this method is that lifetime values measured for the material located under each capacitor can be interpreted by direct examination of defects in that material. Furthermore, this is done without disturbance of the overlying metal or oxide.

The use of the technique in the evaluation of the electrical activity of defects is illustrated in Ref. 3.

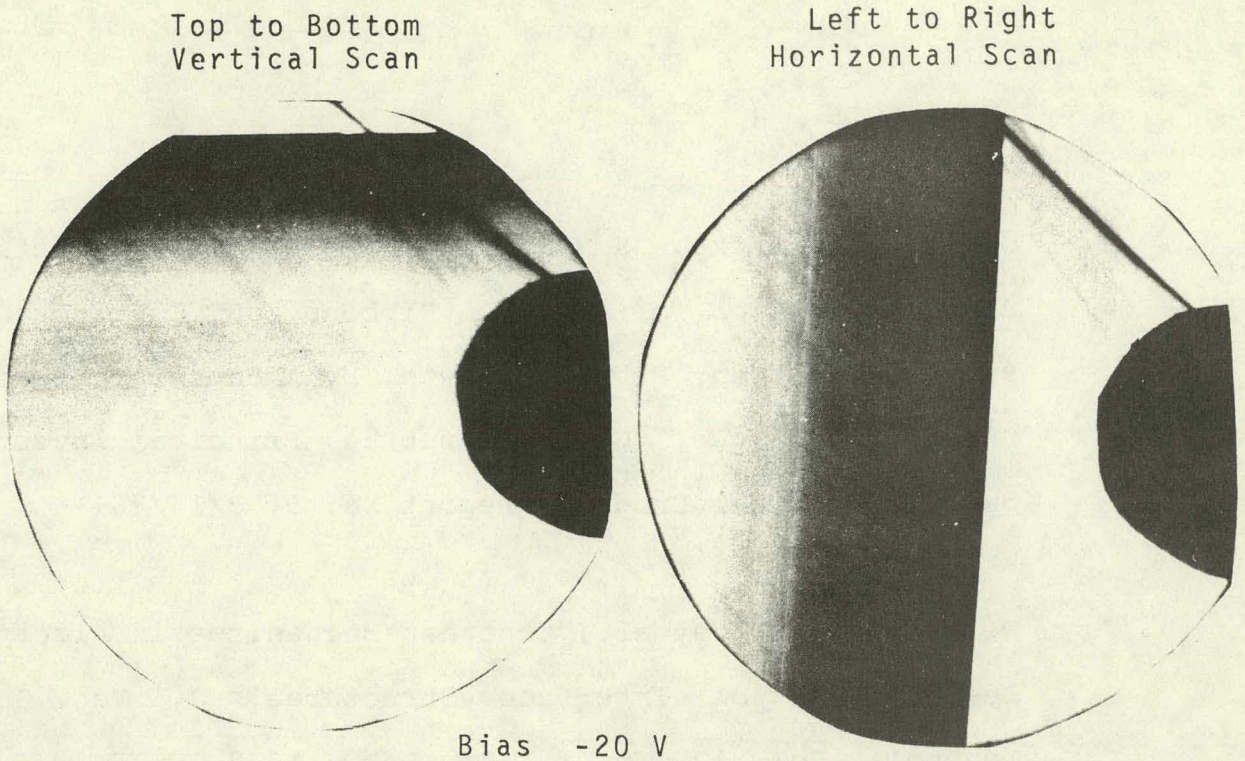

Fig. 9. SEM-EBIC Micrograph of MOS Capacitor Showing Change of Contrast at Oxide Breakdown Points

5.0 ACKNOWLEDGMENT

The original design concept for the 4-probe SEM sub-stage was developed by R. J. Lang, Dept. 454, IBM Research, Yorktown Height, New York.

6.0 REFERENCES

1. G. H. Schwuttke, K. H. Yang, and R. Hezel; Lifetime Characterization of Silicon Ribbons, JPL Contract No. 954144, Silicon Ribbon Growth by A Capillary Action Shaping Technique, G. H. Schwuttke, Principal Investigator, Technical Progress Report No. 5, 9/15/76.

2. W. R. Bottoms, et al., Contrast Mechanisms in Electron Beam Images of Interface Structures, J. Vac. Sci. Technol., Vol. 12, No. 1, Jan./Feb., 1975.

3. K. H. Yang and G. H. Schwuttke, Structural and Electrical Characterization of Silicon Ribbons, JPL Contract No. 954144, Silicon Ribbons Growth by a Capillary Action Shaping Technique, G. H. Schwuttke, Principal Investigator, Technical Progress Report No. 8, 7/1/77.

RIBBON TECHNOLOGY ASSESSMENT: 1976-1986 (PART I)

by

A. Kran

1.0 INTRODUCTION

Czochralski technology represents a well established manufacturing capability. Accordingly, any other silicon sheet technology development program, considered proficient enough to compete with Czochralski technology for $\geq$ \$500/kWE solar array production contracts, must be phased into manufacturing now. Programs not yet ready, should redirect their efforts to capture a share of the post 1986 \$<500/kWE market.

This and our next (final) report will summarize ribbon technology from today's vantage point. We will provide direction for approaching--through ribbon technology--the 1986 \$$\geq$500/kWE solar array energy capacity cost objective. The examination will focus on how to bridge from today's technology development efforts to a specific level of manufacturing competence, using the principles of manufacturing science.

Briefly, manufacturing science is characterized by a systematic effort aimed at narrowing the gap between art and science through automation, computers, and cybernetics. It may be thought of as an action plan for moving technology into full-scale production in a rapid, predetermined manner. As for low-cost sheet, the schedule is already defined, requiring manufacturing technology readiness in the early '80s and a large-scale production capability before '85.

As an application of manufacturing science, consider ribbon growth. If it is to remain a contender for future low cost sheet material, this complex art then must be tranformed, in accordance with the just-mentioned schedule, into a highly automated production system. Such a system would require, in the best case, no more than a "start-stop" pushbutton for operation. In the worst case, it may be permissible for ribbon growth to be initiated by means of a computer-controlled, operator-assisted feedback mechanism.

1.1 Silicon Sheet Technology Status

This silicon ribbon technology analysis seeks to answer the following question: "Assume that the current Czochralski projections (1986: \$24/m^2 sheet material, \$160/kWE, 15% cell, \$10/kg poly) are realistic. Where does ribbon growth stand and how does it compare?"

First, all ribbon technology projections have been reviewed with a hard-nosed attitude to ascertain that feasibility of particular parameter values has been demonstrated or is within reach. Clearly, if ribbon technology is to compete with Czochralski technology for $\geq$500/kWE solar array production contracts through 1986, it must be phased into manufacturing starting in 1978. Otherwise, it will not be ready by 1982, to compete for part of the 30 MW market, or by 1986, to address the 500 MW market. 1982 is considered an intermediate objective leading to the 1986 cost goal. Hence, if $~500/kWE cannot be envisioned with a new sheet technology, then the merits of the technique should be re-evaluated at this time, before a commitment to manufacturing is made.

On the other hand, 1986 projected Czochralski technology must not escape a similar bull-headed scrutiny. We cannot afford to give up on a potential winner, such as ribbon growth, only to find out later, long after the project has been terminated, that Czochralski could not deliver, after all, $500/kWE arrays.

Finally, any future (e.g., 1986) cost objective should be viewed as a goal, not a firm commitment. The important point is to have a number of differing approaches, in order to foster a competitive market environment.

2.0 RIBBON TECHNOLOGY DEFINITION AND PROJECTION

Ribbon technology parameter values were evaluated and projected in conjunction with the following schedule:

A.	Suspension of further Ribbon Technology Development:	1977/78
B.	Definition and Utilization of Manufacturing Science:	1978/86
C.	Initiate Phasing into Manufacturing:	1978
D.	Initial Manufacturing Technology Ready:	1980
E.	Pilot Production:	1980/81
F.	Small Scale Production (1-10 MW):	1982/84
G.	Large Scale Production (20-100 MW):	1985/86

Parameters are listed, for the years 1976, 1978, 1980 in Fig. 1., and for the years 1982, 1984, 1986 in Fig. 2. These data also represent input parameters to our computer simulator of ribbon growth, and are described to the model in terms of four categories:

1. Processing Technology
2. Direct Manufacturing Cost
3. Other Costs (Including Profit)
4. Miscellaneous Category.

LIST OF RIBBON PARAMETERS AND THEIR ASSIGNED VALUES

RIBBON DATA FROM SIMULATIONS 64 65 66 FILE OPENED 11/04/75

YEARS ARE: 1976 1978 1980

```
1  RIBBONS GROWN SIMULTANEOUSLY -     1   1   1
2  RIBBON WIDTH, CM -    5.0 10.0 10.0
3  RIBBON GROWTH RATE,M/HR -    1.32  1.78  2.03 ..OR AS PCT  30  35  40
4  RIBBON THICKNESS, MM -.. 0.40 0.30 0.30
5  YIELD OF  CELL QUALITY  RIBBON, PCT -    70  80  80

  DIRECT COST
6  RIBBON FURNACE, DOLLARS -    50000  50000  50000
7     EQUIPMENT LIFE, YEARS -    7.0  7.0  7.0
8     INTEREST RATE, PERCENT -   10.0 10.0 10.0
9     EQUIPMENT AVAILABILITY, PERCENT -     70   80   80
   PERSONNEL PER SHIFT PER MACHINE
10 11 NO. OF SUPVS -   0.05 0.05 0.05 AT $ -   25000 25000 25000
12 13 NO. OF ENGRS -   0.10 0.10 0.10 AT $ -   20000 20000 20000
14 15 NO. OF TECHN -   0.50 0.25 0.10 AT $ -   10000 10000 10000
16 POLY SILICON COST, DOLS/KG -    65  60  45
17 POLY YIELD TO RIBBON,PERCENT -    80  80  85
   SERVICES AND SUPPLIES
18    CRUCIBLE/DIE/PARTS COST PER DAY -    30  25  25 DOLLARS
19    POWER COST AT -   0.05 0.05 0.05 DOLLARS PER KWH
20    ENERGY TO OPERATE EQUIPMENT -    12  11  11 KW

21 22  O/H -  100 100 100 PCT OF PERS+    25  25  25 PCT OF RAW MATL COST
23  G AND A -    25  25  25 PERCENT OF DIRECT COST+OVERHEAD

24  PROFIT BEFORE TAX, PERCENT - 15 15 15 OF DC+O/H+G&A

  MISCELLANEOUS
25 WORKWEEK, HOURS -  168 168 168
26 CONVERSION EFFICIENCY, PERCENT -    8.00 11.00 12.00
27 ENERGY DENSITY AT AM1,KW/SQ M PEAK -     1   1   1

                                                    13:25:29  SEP 30,1977
```

Fig. 1. Ribbon Technology Parameter Values 1976-1980

LIST OF RIBBON PARAMETERS AND THEIR ASSIGNED VALUES

RIBBON DATA FROM SIMULATIONS 67 68 69 FILE OPENED 11/04/75

YEARS ARE: 1982 1984 1986

```
1  RIBBONS GROWN SIMULTANEOUSLY -     1   1   1
2  RIBBON WIDTH, CM -   10.0 10.0 10.0
3  RIBBON GROWTH RATE,M/HR -    2.28  2.54  3.05 ..OR AS PCT  45  50  60
4  RIBBON THICKNESS, MM -  0.30 0.30 0.30
5  YIELD OF  CELL QUALITY  RIBBON, PCT -    85  90  95

   DIRECT COST
6  RIBBON FURNACE, DOLLARS -    50000  50000  50000
7     EQUIPMENT LIFE, YEARS -    7.0  7.0  7.0
8     INTEREST RATE, PERCENT -   10.0 10.0 10.0
9     EQUIPMENT AVAILABILITY, PERCENT -     80   90   95
   PERSONNEL PER SHIFT PER MACHINE
10 11 NO. OF SUPVS -   0.05 0.05 0.05 AT $ -   25000 25000 25000
12 13 NO. OF ENGRS -   0.10 0.10 0.10 AT $ -   20000 20000 20000
14 15 NO. OF TECHN -   0.10 0.10 0.10 AT $ -   10000 10000 10000
16 POLY SILICON COST, DOLS/KG -    25   15   10
17 POLY YIELD TO RIBBON,PERCENT -    85   90   95
   SERVICES AND SUPPLIES
18    CRUCIBLE/DIE/PARTS COST PER DAY -    25  25  25 DOLLARS
19    POWER COST AT -   0.05 0.05 0.05 DOLLARS PER KWH
20    ENERGY TO OPERATE EQUIPMENT -    11  10   9 KW

21 22  O/H -   100 100 100 PCT OF PERS+   25  25  25 PCT OF RAW MATL COST
23  G_AND_A -    25  25  25 PERCENT OF DIRECT COST+OVERHEAD

24  PROFIT BEFORE TAX, PERCENT - 15 15 15 OF DC+O/H+G&A

   MISCELLANEOUS
25 WORKWEEK, HOURS -   168 168 168
26 CONVERSION EFFICIENCY, PERCENT -   13.00 14.00 15.00
27 ENERGY DENSITY AT AM1,KW/SQ M PEAK -     1   1   1

                                                    13:30:28  SEP 30,1977
```

Fig. 2. Ribbon Technology Parameter Values 1982-1986

Category 1 consist of processing-related parameters, such as ribbon width, where a 10 cm capability is now being demonstrated. We recommend that further development to increase ribbon width beyond 10 cm be postponed until the early '80s, when a viable manufacturing technology is firmly in place. This technology must be fully automated, as it must produce continuous ribbon of excellent quality (15% cell) at a high (95%) yield of "cell quality" material. Other parameters in this category are growth rate (expected to double between 1976 and 1986), and ribbon thickness (unchanged at 0.3 mm).

Category 2 comprises direct cost items, such as crystal growth system cost. As stated in Quarterly Report No. 6 (p. 83), single ribbon growth systems offer the best potential for achieving low-cost silicon ribbon material within the shortest period of time. Such systems can be implemented today through modification of commercially available Czochralski type crystal pullers at a total cost of about $50,000. Sheet-material cost is rather insensitive to variation in capital equipment cost, as can be seen from Fig. 3. Also, since there appears to be no evidence of a substantive program within industry to develop low-cost, reliable ribbon pullers, the $50,000 figure was chosen for the entire time period (1976-1986).

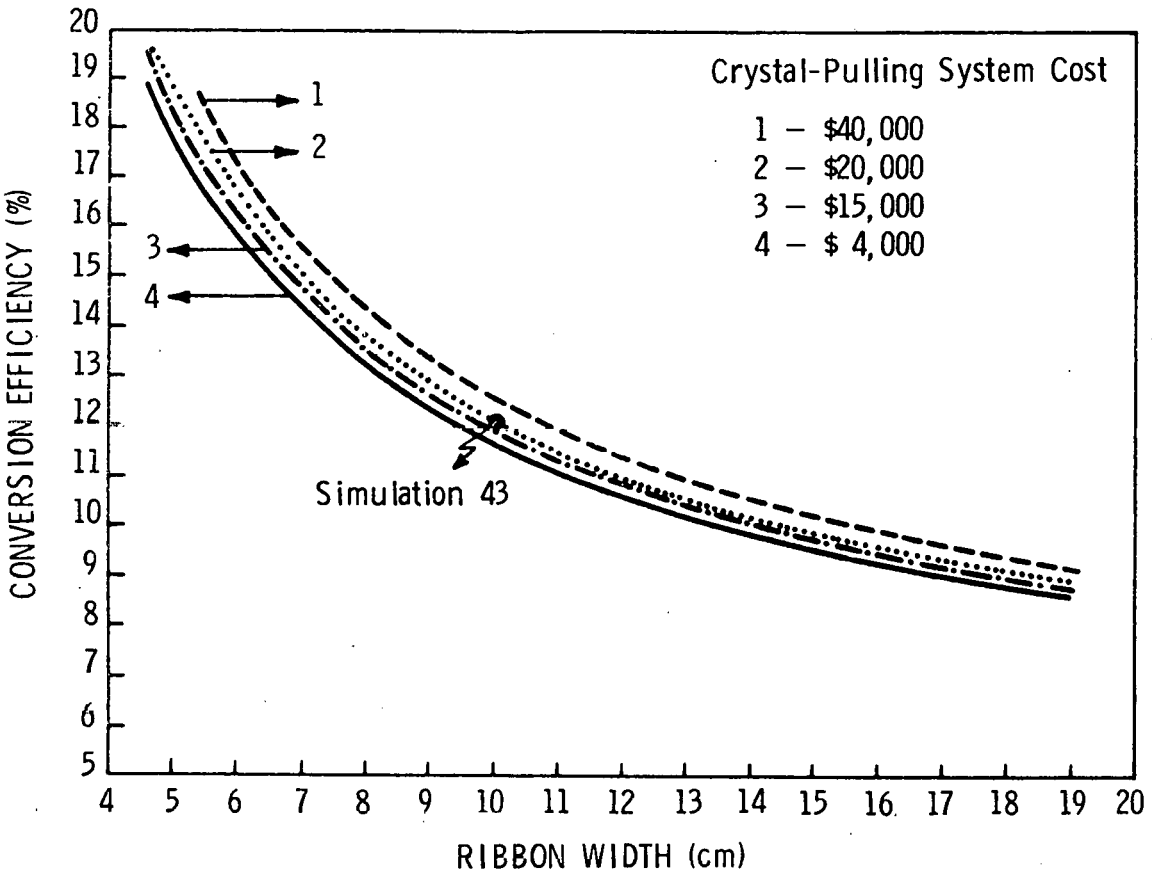

Fig. 3. Future Silicon Ribbon Technology: Conversion Efficiency vs Ribbon Width for Crystal System Costs. (Energy-Capacity Cost, $314/kWE.)

Another key item in category 2 is direct manpower required to keep capital equipment operational. Manpower is allocated on a fractional basis, depending upon the characteristics of the particular ribbon growth system. In 1986, for example, we expect one technician and one engineer to operate and maintain 10 highly automated (95% availability) crystal growth systems. One supervisor will manage 20 production units.

The remaining items are polysilicon cost (JPL projection was used), and the yield of raw material, as it is processed into ribbon form. Because of continuous melt replenishment this yield figure (for 1986) is projected at 95%. Completing this category are services and supplies, consisting of expendable parts, power cost, and the amount of energy required to operate the equipment.

Category 3--overhead, general and administrative expenses, and profit--are defined as percentages relating to other direct-cost-items. These figures have been increased to 100%, 25%, and 15% respectively in order to reflect the operations of larger firms anticipated to enter this business.

Category 4, miscellaneous items, contains the number of hours worked per week, plus solar cell conversion efficiency

(again, JPL's projection was utilized). Also, peak insolation at air mass 1 (on earth), and the economic inflation rate (not used), with 1976 as the base.

As just noted, all costs are in 1976 dollars. The anticipated impact of compounded inflation during the study period (1976-1986) is not included in this report. Although readily computed and integrated into the model, it was decided to exclude the effects of inflation at this time. This was primarily done to enhance the understanding of the model and the relationship between input values and calculated results.

3.0 OUTPUT FROM RIBBON TECHNOLOGY MODEL

Results from this system simulation identify the major elements contributing to sheet material and energy capacity cost. A listing is provided in Figs. 4 and 5, and a percentage analysis in Figs. 6 and 7.

4.0 DISCUSSION OF RESULTS

Our approach to technology projection is "bottoms-up". It consist of first defining, and then projecting, technology (model input) parameters using the production unit concept.

ECONOMICS OF SILICON RIBBON - ONE RIBBON PULLER

SIMUL FILE OPENED 11/04/75

SIMULATION NO:	64	65	66
YEARS:	1976	1978	1980
RIBBONS GROWN SIMULTANEOUSLY	1.00	1.00	1.00
RIBBON WIDTH, CM	5.00	10.00	10.00
AVG YIELDED GROWTH RTE,SQ M/HR	0.03	0.11	0.13
COMBINED YIELD FACTOR	0.56	0.64	0.68
DIRECT COST IN DOLS/SQ METER			
EQUIPMENT CAPITAL RECOVERY	37.84	10.75	9.41
PERSONNEL	127.68	25.29	16.35
POLY SILICON COST	108.18	65.53	46.26
SERVICES/SUPPLIES	40.64	10.41	9.11
SUBTOTAL:	314.34	111.99	81.13
OVERHEAD COST IN DOLS/SQ METER	142.83	35.77	24.22
G&A EXPENSES IN DOLS/SQ METER	114.29	36.94	26.34
PROFIT IN DOLLARS/SQ METER	85.72	27.70	19.75
TOTAL COST IN DOLS/SQ METER	657.17	212.40	151.44
DOLLARS PER KW	8214.68	1930.95	1262.04

Fig. 4. Ribbon Technology Projection 1976-1980

ECONOMICS OF SILICON RIBBON - ONE RIBBON PULLER

SIMUL FILE OPENED 11/04/75

SIMULATION NO:	67	68	69
YEARS:	1982	1984	1986
RIBBONS GROWN SIMULTANEOUSLY	1.00	1.00	1.00
RIBBON WIDTH, CM	10.00	10.00	10.00
AVG YIELDED GROWTH RTE,SQ M/HR	0.16	0.21	0.27
COMBINED YIELD FACTOR	0.72	0.81	0.90
DIRECT COST IN DOLS/SQ METER			
EQUIPMENT CAPITAL RECOVERY	7.87	5.95	4.45
PERSONNEL	13.68	10.34	7.73
POLY SILICON COST	24.19	12.94	7.75
SERVICES/SUPPLIES	7.62	5.81	4.26
SUBTOTAL:	53.36	35.04	24.19
OVERHEAD COST IN DOLS/SQ METER	18.05	12.96	9.48
G&A EXPENSES IN DOLS/SQ METER	17.85	12.00	8.42
PROFIT IN DOLLARS/SQ METER	13.39	9.00	6.31
TOTAL COST IN DOLS/SQ METER	102.66	69.00	48.40
DOLLARS PER KW	789.69	492.83	322.65

Fig. 5. Ribbon Technology Projection 1982-1986

ECONOMICS OF SILICON RIBBON - ONE RIBBON PULLER

SIMUL FILE OPENED 11/04/75

SIMULATION NO:	64	65	66
YEARS:	1976	1978	1980
RIBBONS GROWN SIMULTANEOUSLY	1.00	1.00	1.00
RIBBON WIDTH, CM	5.00	10.00	10.00
AVG YIELDED GROWTH RTE,SQ M/HR	0.03	0.11	0.13
COMBINED YIELD FACTOR	0.56	0.64	0.68
DIRECT COST IN DOLS/SQ METER			
EQUIPMENT CAPITAL RECOVERY	5.76	5.06	6.21
PERSONNEL	19.43	11.91	10.80
POLY SILICON COST	16.46	30.85	30.54
SERVICES/SUPPLIES	6.18	4.90	6.02
SUBTOTAL:	47.83	52.72	53.57
OVERHEAD COST IN DOLS/SQ METER	21.73	16.84	15.99
G&A EXPENSES IN DOLS/SQ METER	17.39	17.39	17.39
PROFIT IN DOLLARS/SQ METER	13.04	13.04	13.04
TOTAL COST IN DOLS/SQ METER	100.00	100.00	100.00
DOLLARS PER KW	8214.68	1930.95	1262.04

Fig. 6. Percentage Analysis--Ribbon Technology Projection 1976-1980

ECONOMICS OF SILICON RIBBON - ONE RIBBON PULLER

SIMUL FILE OPENED 11/04/75

SIMULATION NO:	67	68	69
YEARS:	1982	1984	1986
RIBBONS GROWN SIMULTANEOUSLY	1.00	1.00	1.00
RIBBON WIDTH, CM	10.00	10.00	10.00
AVG YIELDED GROWTH RTE,SQ M/HR	0.16	0.21	0.27
COMBINED YIELD FACTOR	0.72	0.81	0.90
DIRECT COST IN DOLS/SQ METER			
EQUIPMENT CAPITAL RECOVERY	7.67	8.62	9.19
PERSONNEL	13.33	14.98	15.98
POLY SILICON COST	23.56	18.76	16.00
SERVICES/SUPPLIES	7.43	8.42	8.81
SUBTOTAL:	51.98	50.78	49.98
OVERHEAD COST IN DOLS/SQ METER	17.58	18.78	19.59
G&A EXPENSES IN DOLS/SQ METER	17.39	17.39	17.39
PROFIT IN DOLLARS/SQ METER	13.04	13.04	13.04
TOTAL COST IN DOLS/SQ METER	100.00	100.00	100.00
DOLLARS PER KW	789.69	492.83	322.65

Fig. 7. Percentage Analysis--Ribbon Technology Projection 1982-1986

In this concept, labor, capital equipment, and raw material parameters are combined in an organized and systematic way, and presented to the computer model for translation into readily understood economic terms. Results (output) from the model are not "massaged" to meet a given cost objective, but form the basis for subsequent sensitivity, or parameter trade-off, analysis. Sensitivity analysis results in a series of graphs, which permit the reader to form his own opinion regarding the credibility of future technology cost goals.

Figure 8 shows--in graphical form--model output resulting

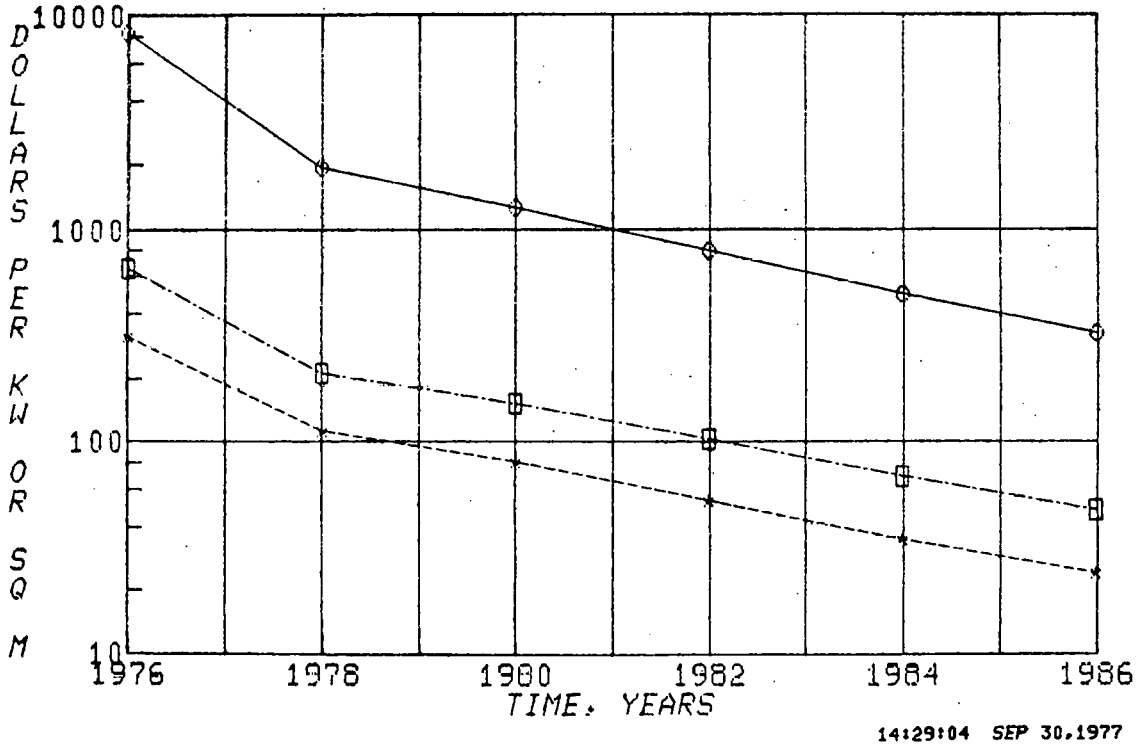

Fig. 8. Photovoltaic Technology Cost Objectives vs Time

from parameter values of Figs. 1 and 2. It represents a semi-log plot of energy capacity cost at the level of silicon sheet material ($/kWE), total sheet cost ($/m^2), and direct costs ($/m^2) respectively versus time (1976-1986). The curves are parallel lines (as expected), and, except for the interval between 1976 and 1978, form straight lines. These lines amount to a projected cost reduction between 1978 and 1986 of a factor of 6 (e.g., $212/m^2 to $48/m^2).

More detail can be gathered from Fig. 9, which is a regular

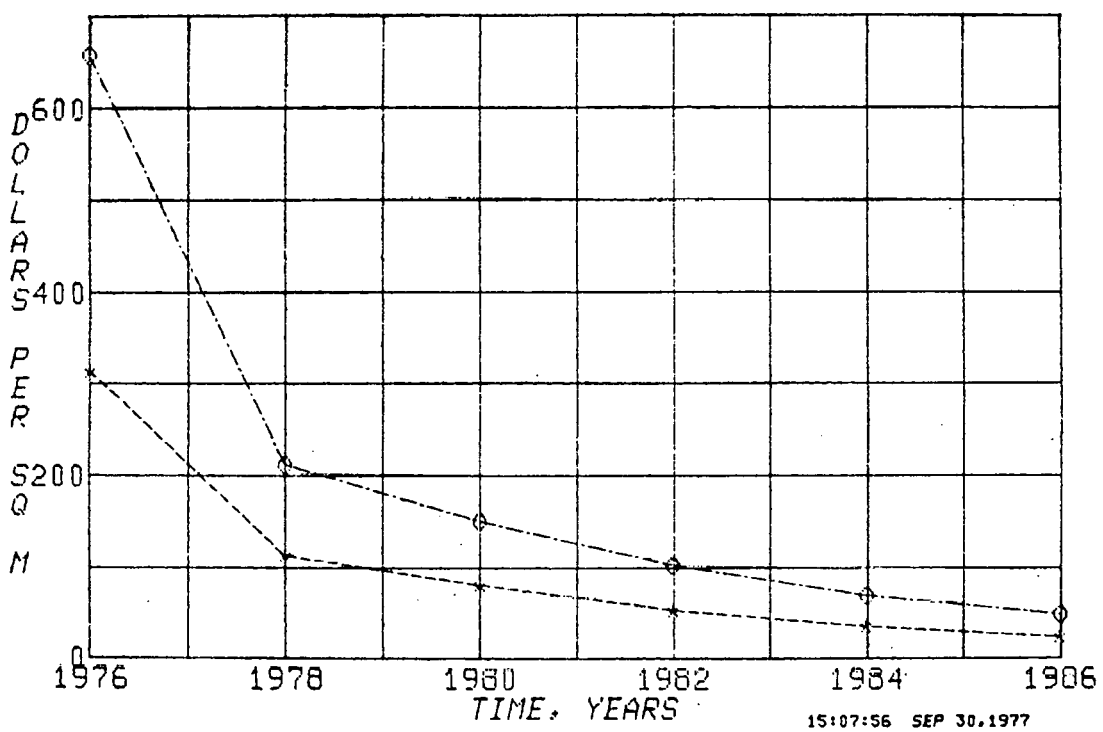

Fig. 9. Silicon Sheet Technology Cost Objectives vs Time

plot of time versus both the total sheet cost ($/m^2) and the direct costs ($/m^2). The most drastic reduction in sheet cost is expected to occur between 1976 and 1978. It is a direct result of increasing ribbon width (5-10 cm) and conversion efficiency (8-11%), plus relatively minor improvements in other parameter values (see Fig. 1). This factor of 3 decrease ($657/m^2 to $212/m^2) is obviously still a hypothetical case. To the best of our knowledge, no manufacturing plant is producing silicon ribbon capable of meeting our 1976-1978 technology definition.

Direct cost items represent 50% of total sheet cost throughout the study period. Direct costs are dominated by labor and polysilicon cost through 1986. At that time, both are still twice the cost of equipment capital recovery and services/supplies. As a result of observing the 1986 cost breakdowns (Fig. 5), we must infer that a $20/m^2 sheet cost is unlikely to occur, using our definition of future ribbon technology.

Figure 10 is a semi-log plot versus time of our projected ribbon costs and those reviewed by JPL at the ERDA Williamsburg Meeting. The JPL figures represent Czochralski-based sheet technology.

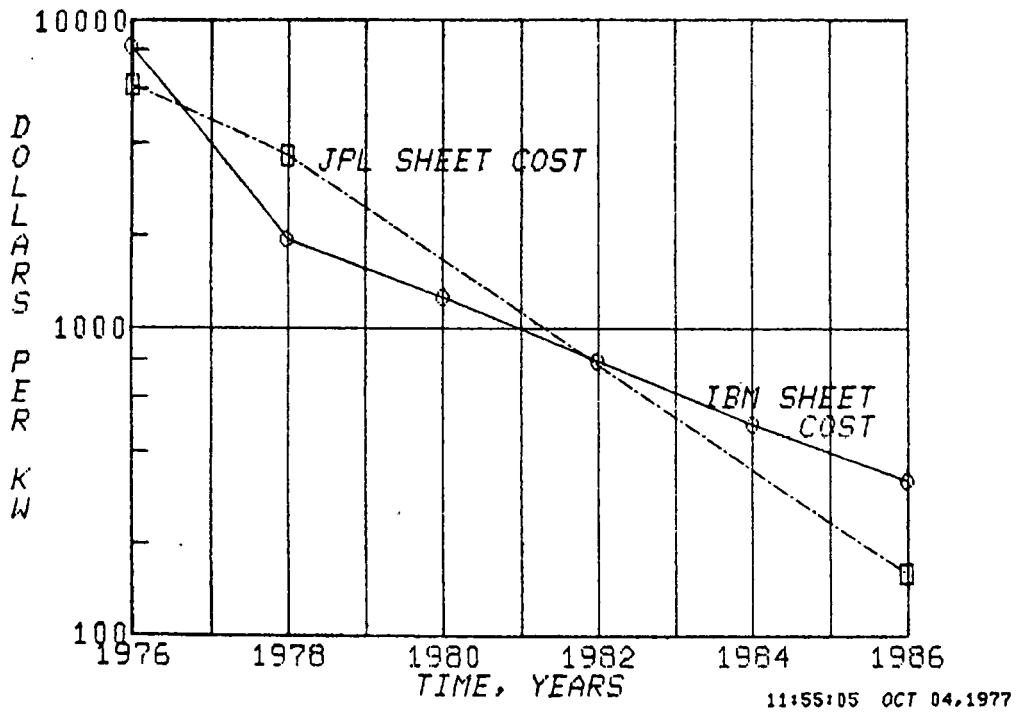

Fig. 10. Photovoltaic Technology Cost Objectives vs Time

The difference between the curves might be attributed to the prevailing difference in status of these two technologies:

Czochralski: Mature technology. Continued pressure to reduce product cost in view of increasing volume.

Ribbon: New technology. Development frozen at 10 cm width for immediate conversion to manufacturing technology. Steady cost improvements, but insufficient throughput capability for spectacular gains.

Next, through sensitivity analysis, technology parameters required to achieve low cost (~ $\$20/m^2$) sheet objectives will be studied further.

5.0 SENSITIVITY ANALYSIS

A simple, yet effective technique has been developed for sensitivity analysis. It allows the analyst to test the sensitivity of two technology parameters (e.g., polycost and ribbon width), while holding all other model parameters constant. For instance, assume that we want to test the 1986 sheet cost of $\$48.40/m^2$ for possible reduction to $\$20/m^2$ by varying projected poly cost ($10/kg) and ribbon width (10 cm). This is accomplished in the computer program by establishing parameter limits. (Poly cost: $4-25/kg; Ribbon Width: 4-25 cm).

Specific parameter values required for each computer calculation are obtained by stochastically sampling between

these limits first, and then calculating the resultant energy-capacity cost at the level of silicon sheet material. Only those parameter values that result in the specified sheet material cost (e.g., Table I, $30.00, ± 0.5%)[1] are accepted as valid data points. All others are rejected. The model is iterated until the relationship (if one exists) between the input parameter and the specified output (dollars/m^2) is determined.

Table I lists the data points generated for the bottom curve

Table I. Data points for $30/$m^2$ curve

Item No.	Iteration	Poly Cost ($/kg)	Ribbon Width (cm)	Sheet Cost ($/$m^2$)	Energy Capacity Cost ($/KWE)
1	76	11.56	24.37	30.01	200.08
2	542	6.73	16.60	30.09	200.57
3	557	4.21	14.20	30.03	200.17
4	607	9.67	20.80	29.88	199.16
5	871	5.26	15.13	30.11	200.74
6	1195	10.93	22.90	30.07	200.44
7	1415	11.14	23.32	30.08	200.54
8	1530	10.30	21.64	30.09	200.59
9	1565	8.41	18.70	30.03	200.21
10	2165	4.84	14.92	29.86	199.07
11	2540	10.51	22.27	29.92	199.48
12	2834	7.15	17.23	29.89	199.30
13	3073	4.42	14.50	29.96	199.74
14	3246	9.04	19.54	30.09	200.62
15	3721	7.57	17.65	29.99	199.92
16	3724	10.30	21.64	30.09	200.59
17	3985	11.56	24.16	30.14	200.91
18	4125	7.15	17.23	29.89	199.30
19	4599	5.26	15.13	30.11	200.74
20	4629	8.62	18.91	30.11	200.74

(1) The ± 0.5% spread in specified sheet material cost is used to limit the number of computer iterations of the model.

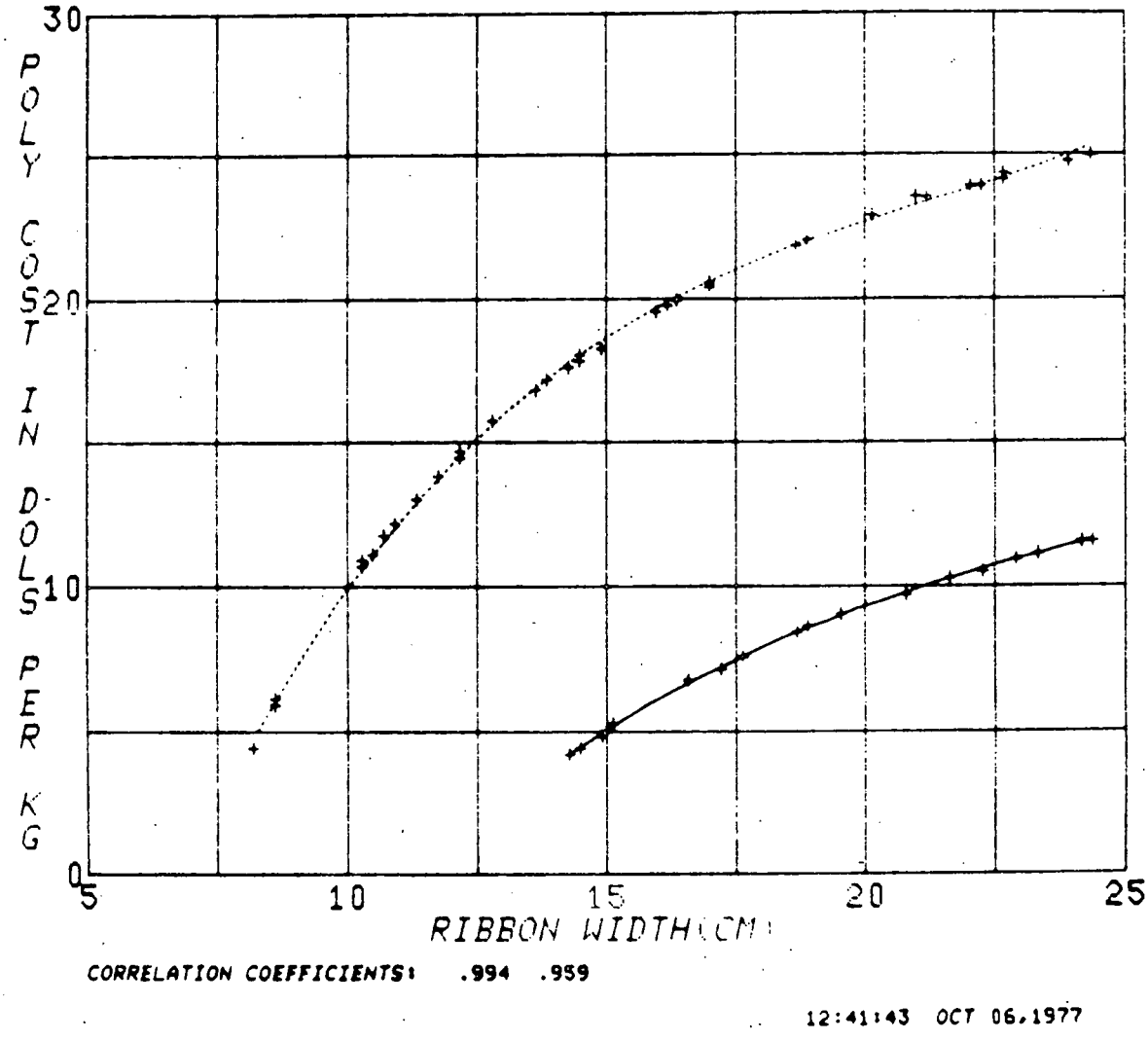

Fig. 11. 1986 Sheet Technology (Poly Cost vs Width)

of Fig. 11. These data points define the particular relationship between polysilicon cost and ribbon width, which results in a sheet material cost of $\$30/m^2 \pm 0.5\%$. (All other model input parameters are as shown for 1986 in Fig. 2.) The two curves of Fig. 11 are least-squares fit (third order polynomial). It might be of interest to note

that it took 4629 iterations of the model (~ 4 minutes of CPU time) to gather 20 data points.

In addition to the $\$48/m^2$ and $\$30/m^2$ curves, a third relationship between poly cost and ribbon width was sought, which was to result in a sheet material cost of $\$20/m^2$.

After 8461 iterations, only one data point (Poly cost: $4.42, Ribbon Width: 24.79 cm) was identified, and the computer run was terminated. Hence, we conclude that a sheet material cost of $\$20/m^2$ is highly unlikely with this set of technology parameter values. However, a $\$30/m^2$ sheet material cost level can be obtained with $5/kg poly, 15 cm wide ribbon, or $10/kg poly, 21 cm wide ribbon.

6.0 CONCLUSIONS

1. If ribbon technology is to compete with Czochralski technology for $\$\geq 500/kW_E$ solar array production contracts through 1986, it must be phased into manufacturing starting in 1978.

2. The following schedule is proposed for bridging from ribbon technology development to large scale production through utilization of manufacturing science:

A.	Suspension of further Ribbon Technology Development:	1977/78
B.	Definition and Utilization of Manufacturing Science:	1978/86
C.	Initiate Phasing into Manufacturing:	1978
D.	Initial Manufacturing Technology Ready:	1980
E.	Pilot Production:	1980/81
F.	Small Scale Production (1F.10 MW):	1982/84
G.	Large Scale Production (20-100 MW):	1985/86

3. For 1986, the following sheet technology costs are projected. They are based upon the schedule (item 2), technology parameter values of Fig. 2 on page 68, and have been taken from Fig. 11 on page 81:

   A. $\$48/m^2$ ($320/kWE) sheet material cost appears as a good bet for 10 cm wide ribbon, $10/kg poly, 15% cell.

      Alternatives: 16.3 cm wide ribbon, $20/kg poly
      8.5 cm wide ribbon, $ 5/kg poly

   B. $\$30/m^2$ ($200/kWE) sheet material cost cannot be obtained with 10 cm wide ribbon, 15% cell, even at zero poly cost.

      Possibilities: 21.0 cm wide ribbon, $10/kg poly
      15.0 cm wide ribbon, $ 5/kg poly

C. $20/m^2$ ($133/kWE) sheet material cost is unrealistic with ribbon technology defined here and considered reasonable.

Data Point: 25.0 cm wide ribbon, $4/kg poly.

4. Further ribbon technology development beyond 10 cm width should be postponed until the early 1980(s), when a viable manufacturing technology, capable of producing high quality ribbon (15% cell), is firmly in place.

5. Future cost of single-ribbon pulling systems has been revised upward to $50,000. Since there appears no evidence of a substantive program within industry to develop such equipment (must also be highly reliable, and automated), there is concern over meeting even that objective.

☆U.S. GOVERNMENT PRINTING OFFICE: 1978-740-094/1267